ACTA
PROTOZOOLOGICA

Special issue:
Protists as Bioindicators of Past
and Present Environmental Conditions

Acta Protozool. (2013) 52: 161–180
http://www.eko.uj.edu.pl/ap
doi:10.4467/16890027AP.13.0015.1112

Benthic and Planktic Foraminifera as Indicators of Late Glacial to Holocene Paleoclimatic Changes in a Marginal Environment: An Example from the Southeastern Bay of Biscay

Jennifer GARCIA[1], Meryem MOJTAHID[1], Hélène HOWA[1], Elisabeth MICHEL[2], Ralf SCHIEBEL[1], Céline CHARBONNIER[3], Pierre ANSCHUTZ[3] and Franciscus J. JORISSEN[1]

[1]UMR CNRS 6112 LPGN-BIAF – Laboratoire des Bio-Indicateurs Actuels et Fossiles, LUNAM Université, Université d'Angers, Angers, France; [2]UMR CNRS-CEA 8212 LSCE – Laboratoire des Sciences du Climat et de l'Environnement, LSCE-Vallée, Gif-Sur-Yvette, France; [3]UMR CNRS 5805 EPOC – Environnements et Paléo-environnements OCéaniques, Site de Talence, Université de Bordeaux 1, Talence, France

Abbreviations: AABW – Antarctic Bottom Water; BoB – Bay of Biscay; ENACW – Eastern North Atlantic Central Water; HTM – Holocene Thermal Maximum; IPC – Iberian Poleward Current; MOW – Mediterranean Outflow Water; NAO – North Atlantic Oscillation; NH – Northern Hemisphere; NEADW – North East Atlantic Deep Water; NC – Navidad Current; SE – Southeastern; SST – Sea Surface Temperatures.

Abstract. Benthic and planktic foraminiferal assemblages from two sediment cores (2,000 m depth, 44°33′N, 2°45′W) were analyzed to first compare modern and dead faunas and next to study changes in the hydrology of the southeastern Bay of Biscay (SE BoB) over the last 12.8 cal ka BP. Considering benthic ecosystem characteristics, the first part of the paleorecord (12.8–7.6 cal ka BP) is composed of laminated sediments that may have resulted from turbiditic overflow events, whereas occurrences of transported species (e.g. *Nonionella* sp., *Cassidulina carinata*) attest of continental influence at the core location. After 7.6 cal ka BP, the sediment becomes bioturbated concomitantly to the stabilization of the sea-level. The benthic foraminiferal fauna is largely dominated by *Uvigerina peregrina* suggesting a high seasonality with seasonal pulsed organic matter fluxes to the seafloor. On the other hand, the planktic foraminiferal composition indicates that surface water masses were under the influence of the polar front in the early record, which retreated at about 11.5 cal ka BP. The early Holocene is characterized by relatively warm and stratified water masses at 8.4–4.8 cal ka BP. The last 4.8 cal ka BP records a gradual sea surface water cooling trend and enhanced foraminiferal production from ~ 2.6 cal ka BP until present. The early (12.8–10.5 cal ka BP) and late (2.3–1.7 cal ka BP) Holocene are characterized by the presence of the planktic species *Globigerinoides ruber* probably caused by intrusions of the Iberian Poleward Current (IPC), and a negative state of the North Atlantic Oscillation (NAO).

Key words: Benthic foraminifera, planktic foraminifera, stable isotopes, Bay of Biscay, Holocene, Iberian Poleward Current (IPC).

Address for correspondence: Jennifer Garcia, UMR CNRS 6112 LPGN-BIAF – Laboratoire des Bio-Indicateurs Actuels et Fossiles, LUNAM Université, Université d'Angers, 2 Boulevard Lavoisier, 49045 Angers Cedex, France; E-mail: jenifer.garcia@univ-angers.fr

INTRODUCTION

Over the last 12.8 cal ka BP, the Northern Hemisphere (NH) underwent several climate changes. The Younger Dryas cooling event (YD – 12.8–11.5 cal ka BP – Broecker *et al.* 2010) may have resulted from the collapse of the North American ice sheets leading to a dramatic freshwater input into the North Atlantic (e.g. Fahl and Stein 2012). The ensuing Holocene period was for a long time considered climatically stable (e.g. Dansgaard *et al.* 1993). Recently, this oversimplification has been questioned (e.g. Oldfield 2003), since evidence for Holocene variability at centennial to millennial timescales has been provided by both oceanic and terrestrial proxy records (e.g. Bond *et al.* 2001, Oppo *et al.* 2003, Mayewski *et al.* 2004, Debret *et al.* 2009). The frequently quoted mechanisms to explain Holocene climatic modulations are the ocean and atmospheric circulations, as well as the solar radiative budget (e.g. Bond *et al.* 2001). Other potential controls (e.g. hydrological cycles, sea level, sea ice extent, vegetation cover and human impact) are also believed to play a role in Holocene variability (e.g. Ruddiman and Ellis 2009). The Holocene period has been broadly divided into three major climatic phases as defined by Andersen *et al.* (2004): 1) a general warming period (11.5–9.5 cal ka BP), 2) the Holocene Thermal Maximum period (HTM; 9.5–6.5 cal ka BP), and 3) a final late Holocene cooling period (6.5–0 cal ka BP). The first phase can be correlated to the high summer insolation in the NH, which reached its maximum at approximately 11 cal ka BP due to a maximum of both precession and obliquity (e.g. Wanner *et al.* 2008). However, until about 9 cal ka BP, a large remnant ice sheet persisted in North America (e.g. Kaufman *et al.* 2004). The HTM corresponds to a period of continuing high summer insolation, the North American ice sheet becoming too small to affect the climate on a global scale (e.g. Wanner *et al.* 2008). The following global late Holocene cooling period corresponds to the declining summer insolation in the NH (e.g. Wanner *et al.* 2008).

Marine sedimentary archives from continental margins are suitable to describe Holocene climatic changes. They offer the opportunity to record both marine and continental influences, and to trace global and regional forcing signals. The Bay of Biscay (BoB) is an appropriate location to track Holocene climatic changes, because this marginal oceanic embayment records oceanic circulation patterns in Northeastern (NE) Atlantic. This is mainly due to the location of the BoB under the alternating influence of the Azores High and the Icelandic Low pressure system on the one hand, and in the transitional area between subtropical and temperate marine biogeographic provinces on the other hand (Longhurst 2007).

The BoB has been largely investigated in terms of modern hydrology and sedimentary processes (e.g. Le Cann and Serpette 2009, Schmidt *et al.* 2009, Mouret *et al.* 2010, Kuhnt *et al.* 2013). The ecology of modern benthic foraminifera has been extensively studied (see review in Mojtahid *et al.* 2010), and the ecology of modern planktic foraminifera has been investigated with a focus on effects of the adjacent continent, i.e. river runoff and sediment reworking (Retailleau *et al.* 2009, 2011, 2012). However, until now, only few studies have focused on Holocene climatic variability recorded in the open slope environments of the BoB. Caralp (1971) established the late Quaternary stratigraphic framework (Late Pleistocene–Holocene) for the area. More recently, Mojtahid *et al.* (2013) have investigated a high resolution sediment record covering the last 9 cal ka BP, collected at a 550 m water depth site in the southeastern BoB (Station B; Fig. 1). Five main climatic phases were described on the basis of changes in planktic and benthic ecosystems. These climatic phases were related to modifications in local oceanic circulation, controlled by the North Atlantic Oscillation (NAO) and changes in the adjacent river runoff, whereas orbital forcing variations overprint these parameters (Mojtahid *et al.* 2013). The present study is an attempt to improve the understanding of the past 12.8 cal ka BP climate history in the marginal BoB, by investigating the spatial continuity of the climate signals recorded at Station B (Mojtahid *et al.* 2013). We will do so by studying a more offshore site in the BoB (Station WH, 2,000 m water depth, 115 km off the French coast; Fig. 1).

To achieve this specific objective, a long Kullenberg core (CADIAC WH; Station WH), covering the last ~ 12.8 cal ka BP, was studied by combined sedimentological, microfaunal (planktic and benthic foraminifera), and stable isotope analyses. In addition, a short sediment core, with an undisturbed sea water/sediment interface, was recovered at the same site (Core FC WH). In this sedimentary record, covering the last ~ 1.2 cal ka BP at high resolution, living (stained) and dead foraminiferal assemblages were compared to investigate to what extent the ecological characteristics of the recent faunas are inscribed in the fossil record.

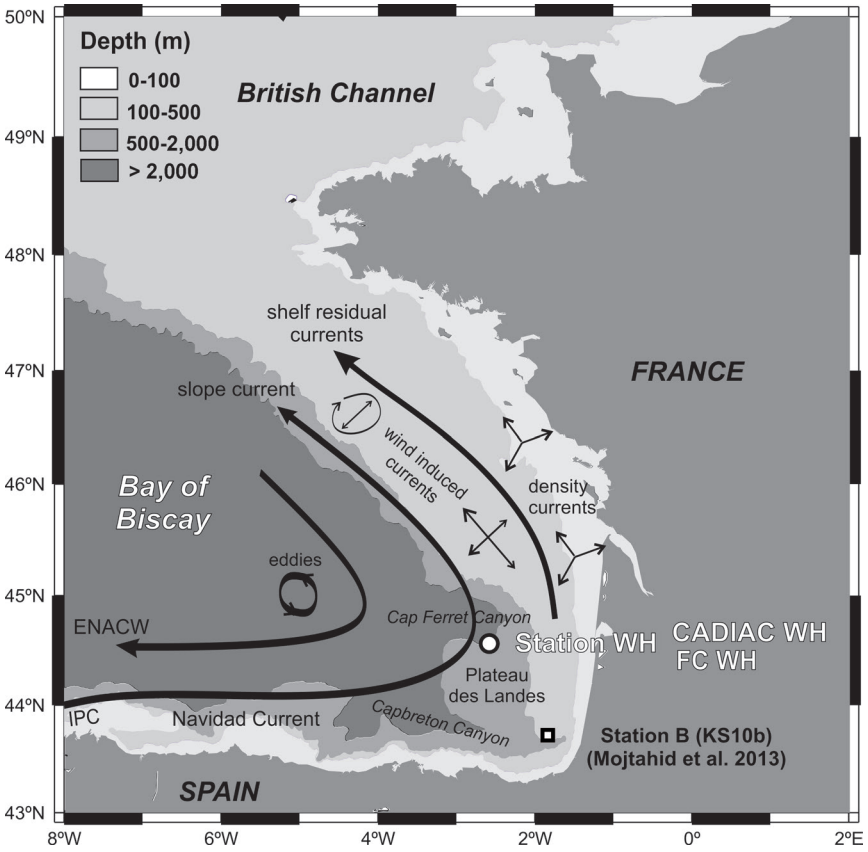

Fig. 1. Study area bathymetry (Liu and Dittert 2010), surface circulation patterns (Koutsikopoulos *et al.* 1996), and location of the study Site WH (44°33′N, 2°45′W; 2,000 m water depth). The position of Site KS10b (Mojtahid *et al*. 2013) is marked by a white square. IPC – Iberian Poleward Current, ENACW – Eastern North Atlantic Central Waters.

STUDY AREA

The BoB is a marginal oceanic embayment bordered to the east by the French coast, and to the south by the Spanish coast. Our 2,000 m deep sampling site is located in the SE BoB at the northern limit of the Plateau des Landes, 1,000 m above the channel axis of the Cap Ferret canyon (Fig. 1). At this site location, sediments consist mainly of hemipelagic deposits (Faugères *et al.* 2002). The modern sediment accumulation rate, obtained by ^{210}Pb profile measurements, is approximately 28 mg cm^{-2} a^{-1} (Schmidt *et al.* 2009).

Surface circulation

The western BoB is characterized by an anticyclonic surface circulation influenced by the Eastern North Atlantic Central Water (ENACW) (Koutsikopoulos and Le Cann 1996) (Fig. 1). Slope Water Oceanic eDDIES (SWODDIES) can develop from jet-like extensions of the poleward slope current off northern Spain and the Armorican shelf-break (Pingree and Le Cann 1992). Because of its mid-latitude position, the hydrography of the BoB is subjected to a strong seasonality. In early winter (December/January), the Iberian Poleward Current (IPC) follows the Iberian shelf-break in a northward direction, and may expand into the SE BoB where it is named the Navidad Current (NC) (Fig. 1). The NC induces intrusions of warm and saline waters (Durrieu de Madron *et al.* 1999; van Aken 2002) when weak northerly winds intersperse with strong south-south-westerly winds (e.g. Garcia-Soto *et al.* 2002, Le Cann and Serpette 2009). Based on satellite data from 1985, incursions of the IPC into the BoB have been correlated to negative NAO phases (Decastro *et al.* 2011). The SE

BoB is also strongly affected by freshwater discharge from the SW French estuaries (Gironde, Adour), leading to seasonal fluctuations in salinity, turbidity and nutrient discharges in surface waters (Puillat *et al.* 2004).

Water masses

Four main water masses can be differentiated in the BoB (van Aken 2000a, b, 2001): 1) From the seafloor to ~ 3,000 m, the Antarctic Bottom Water (AABW) is present; 2) Above the AABW, the North East Atlantic Deep Water (NEADW) is observed. This water mass is a mixture of other water masses such as the Iceland/Scotland Overflow Water, the Labrador Sea Water or the Lower Deep Water; 3) The highly saline Mediterranean Outflow Water (MOW) occurs between ~ 1,300 and 700 m water depth; 4) The MOW is overlain by the ENACW up to the surface mixed layer. Additionally, the proximity to the continental slope results in the presence of diapycnal mixing layers within the different water masses (Durrieu de Madron *et al.* 1999).

MATERIAL AND METHODS

Station WH (44°33N 2°45W; 2,000 m water depth) was sampled in June 2006 and 2009 during the oceanographic cruises PECH 1 and CADIAC, respectively, onboard the French R/V *Côtes de la Manche*. Two sediment cores were collected at Station WH (Fig. 1). A 85 cm long sediment core (CADIAC WH; 70.84 cm² core surface) was collected using a short Kullenberg piston corer, and a 20 cm long interface core (FC WH; 70.84 cm² sediment surface) was obtained with a multicorer. The sediment/water interface is undisturbed in Core FC WH whereas surface sediment loss from the Kullenberg core is estimated at ~ 4 cm (~ 0.6 ka) by a peak to peak correlation of fossil foraminiferal abundances between the two cores. Radiocarbon dating was performed by UMS-ARTEMIS (Pelletron 3MV) AMS facilities (CNRS-CEA Saclay, France), following the standard procedure described by Tisnérat-Laborde *et al*. (2001). AMS ^{14}C ages were converted to calendar years using the depositional model of the OxCal 4.1 software (Bronk Ramsey 2008) and the IntCal09 calibration curve (Reimer *et al.* 2009), after applying a 360 ± 40 yrs BP reservoir age correction (average value from the global database inhttp://calib.qub.ac.uk/marine/index.html). The age of the surficial sediment of Core FC WH was converted into calendar years using the Bomb04NH1 calibration curve (North of 40°; Hua and Barbetti 2004) instead of IntCal09. The age model of Station WH was constructed by the combination of seven radiocarbon dates (2 for FC WH and 5 for CADIAC WH) obtained for the planktic foraminiferal species *Globigerina bulloides* and *Globorotalia inflata* (Table 1; Fig. 2a).

The sedimentological characteristics were derived from visual description and X-ray analyses obtained with a SCOPIX image processing tool for Core CADIAC WH (Migeon *et al.* 1998). In addition, grain size analyses were performed on Core CADIAC WH using a laser diffractometer Malvern™ Masterizer (Fig. 2b).

For planktic and benthic foraminiferal assemblages, 18 samples were analyzed from Core FC WH (every 0.5 to 4 cm), and 20 samples from Core CADIAC WH (every 2.5 to 5 cm spacing, see Table 2). For each sample, a known volume of sediment was processed. All samples were washed over a 150 µm mesh. Living (Rose Bengal stained; Walton 1952) foraminiferal individuals were analyzed only for Core FC WH (wet picked). Non transparent agglutinated and miliolid tests were broken in order to inspect their coloration. The fossil fauna were dry picked. When necessary, samples were split using a microsplitter, and at least 250 individuals were picked from entire splits for benthic as well as planktic foraminifera (see review in Murray 2006). The standing stock of the live benthic fauna was standardized to a 50 cm² surface. The number of fossil individuals was calculated per gram of dry sediment. The dry sediment weight (W_d) was calculated following the formula $W_d = V_w (1 - \varphi) 2.65$, with φ being the sediment porosity measured on parallel cores recovered simultaneously, V_w (cm^3) being the initial sample volume, and 2.65 (g cm^{-3}) being the average bulk density (Berner 1980).

Table 1. Radiocarbon dating, calibrated ages (cal ka BP) and their corresponding depths in Core FC WH (in bold) and Core CADIAC WH. Dates in Core CADIAC WH are corrected for the 4 cm surface sediment loss.

Depth (cm)	Age ^{14}C (ka BP)	pMC corrected fractionation	Material	Calibrated Age (cal ka BP)	1/σ	
					Limit	Limit
				(Reservoir Age = 360 ± 40 yrs)	–	+
0.25	–	**1.025 ± 0.34**	***G. bulloides*; *G. inflata***	**–0.046**	**0.006**	**0.021**
4.5	1.065 ± 40	0.8756 ± 0.46	*G. bulloides*	0.636	0.260	0.249
18	**1.590 ± 30**	**0.8204 ± 0.28**	***G. bulloides*; *G. inflata***	**1.156**	**0.156**	**0.134**
59.5	2.840 ± 30	0.7024 ± 0.21	*G. bulloides*	2.639	0.192	0.227
74.5	5.460 ± 35	0.5069 ± 0.23	*G. bulloides*	5.693	0.176	0.186
79.5	9.340 ± 45	0.3126 ± 0.17	*G. bulloides*	10.215	0.173	0.144
84.5	11.300 ± 50	0.2449 ± 0.15	*G. bulloides*	12.815	0.150	0.165

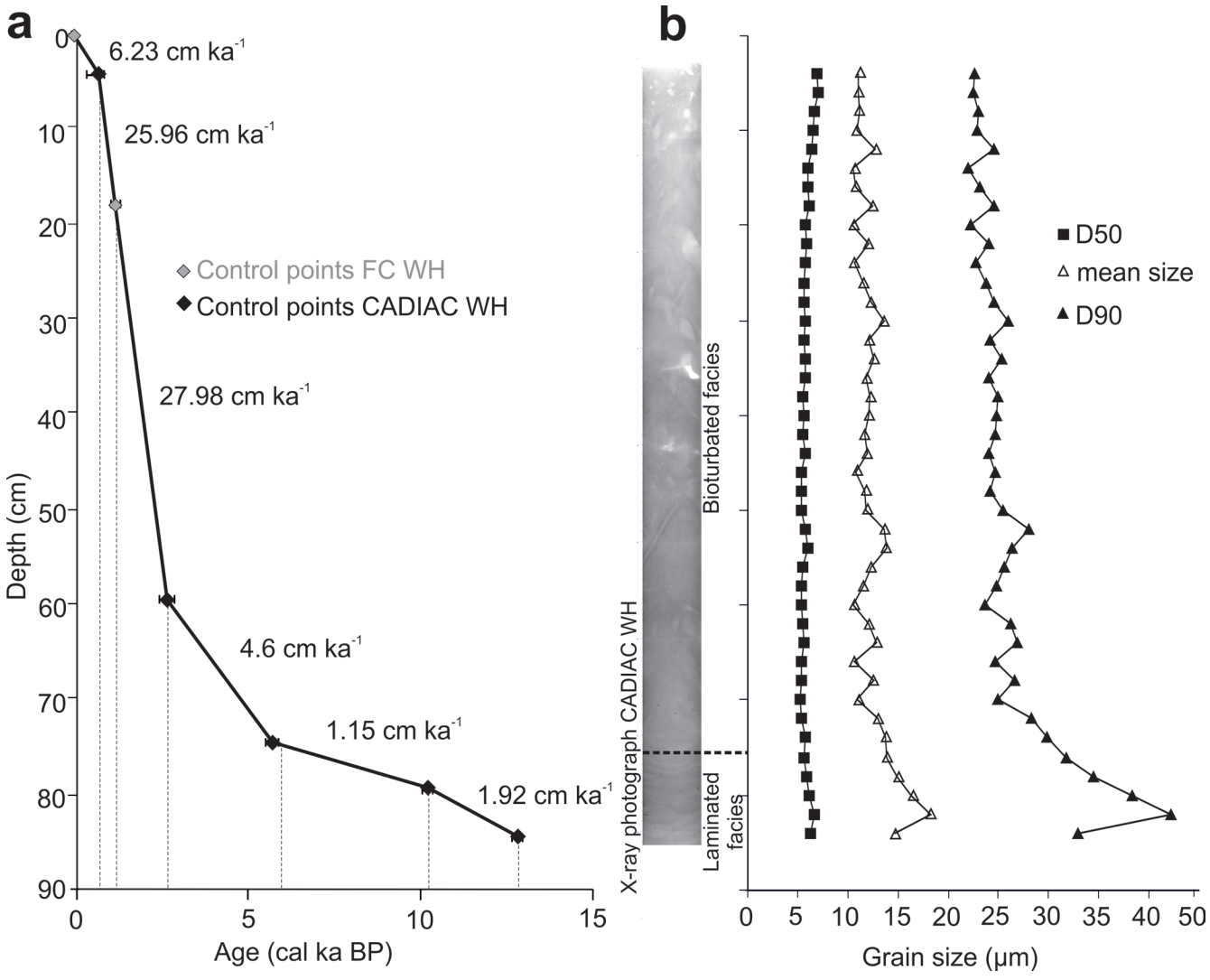

Fig. 2. a – age model and AMS radiocarbon ages for Cores FC WH and CADIAC WH; **b** – X-Ray photograph of Core CADIAC WH and grain-size parameters.

Planktic and Benthic Foraminiferal Accumulation Rates (PFAR and BFAR) are expressed as number of individuals cm^{-2} ka^{-1} (Herguera and Berger 1991). In the fossil record, agglutinated benthic foraminifera only found in the topmost 5 cm, are considered as non-fossilizing (Bizon and Bizon, 1984) and are not taken into account for the calculation of percentages.

Neogloboquadrina incompta encompasses different morphotypes from *N. incompta sensu stricto* (the same as the morphotype *N. pachyderma* dextral) to the pachyderma-dutertrei (P-D) intergrade morphotype (Darling and Wade 2008).

For oxygen and carbon stable isotopes measurements, both for *G. inflata* and *G. bulloides*, 10 to 20 individuals were hand-picked every 0.5 to 5 cm from the 250–315 µm size fraction (Fig. 5). Analyses were performed at LSCE, Gif-sur-Yvette, using 3 types of mass spectrometers (VG-Optima Isoprime and Δ+ mass spectrometers) coupled with a Carbo Prep preparation h line. Stable isotope ratios are expressed in ‰ versus VPDB (Vienna Pee Dee Belemnite standard), defined with respect to NBS19 calcite standard (Coplen 1988). The mean external reproducibility (1 σ) of carbonate standards is ± 0.05‰ and 0.06‰ for $\delta^{13}C$ and $\delta^{18}O$, respectively.

RESULTS

Sedimentological characteristics

Core FC WH consists of 20 cm (~ 1.2 cal ka BP) bioturbated light grey soft clays. The 85 cm long Core CADIAC WH covers the last ~ 12.8 cal ka BP. From ~ 12.8

to 7.6 cal ka BP, the X-ray photograph (Fig. 2b) reveals ~ 9 cm of fine laminated layers corresponding to a period of low sedimentation rates (~ 1.15–1.92 cm ka^{-1}, Fig. 2a). Without any erosional contact, after 7.6 cal ka BP, sediments become bioturbated and sedimentation rates increase, to vary from ~ 4.6 to 28 cm ka^{-1}. The median grain size (D50) does not show a clear pattern throughout the core (Fig. 2b). However, the mean grain size and the D90 show coarser sediment (silty-clayey) in the laminated facies (85–76 cm; mean grain size ~ 15 µm; D90 ~ 35 µm) than in the bioturbated facies (76–4 cm; mean grain size ~ 11 µm; D90 ~ 24 µm).

Foraminiferal analyses

Comparison between living (stained) and dead-fossil benthic foraminifera in the 20 cm long Core FC WH

The total standing stock of the living (stained) benthic foraminifera in Core FC WH (0–20 cm) is ~ 250 ind. 50 cm^{-2}. The average living depth (ALD_{10}, calculated according to Jorissen *et al.* 1995) of the total living benthic foraminiferal fauna is 1.02 cm. Absolute densities rapidly decrease downward from ~ 180 ind. 50 cm^{-3} in the upper 0.5 cm to 3 ind. 50 cm^{-3} at 4.5 cm. No living individuals are found below 6 cm (Fig. 3a). The species richness (number of species) in the living fauna decreases with depth, from a maximum of 20 species at 0.5–1 cm to 3 at 4–5 cm (Fig. 3b). The living fauna is dominated by calcareous hyaline species (~ 85.9%). Agglutinated species represent ~ 8.5% and porcelaneous species account for ~ 5.5% of the total fauna. The main species are in descending order: *Hoeglundina elegans* (~ 54.4%), *Cibicidoides kullenbergi* (~ 8.0%), *Uvigerina peregrina* (~ 6.3%), *Gyroidina orbicularis* (~ 5.5%), and *Gavelinopsis translucens* (~ 5.2%). Minor species like *Bulimina inflata*, *Eggerella bradyi*, *Pyrgo murrhina*, and *Sigmoilospsis schlumbergeri* each account for less than 5% of the total living assemblage (Fig. 3a; Table 2).

The average density of dead-fossil benthic foraminifera in the 20 cm long Core FC WH is ~ 3,600 ind. 50 cm^{-3} (Fig. 3c; Table 2). Absolute abundances

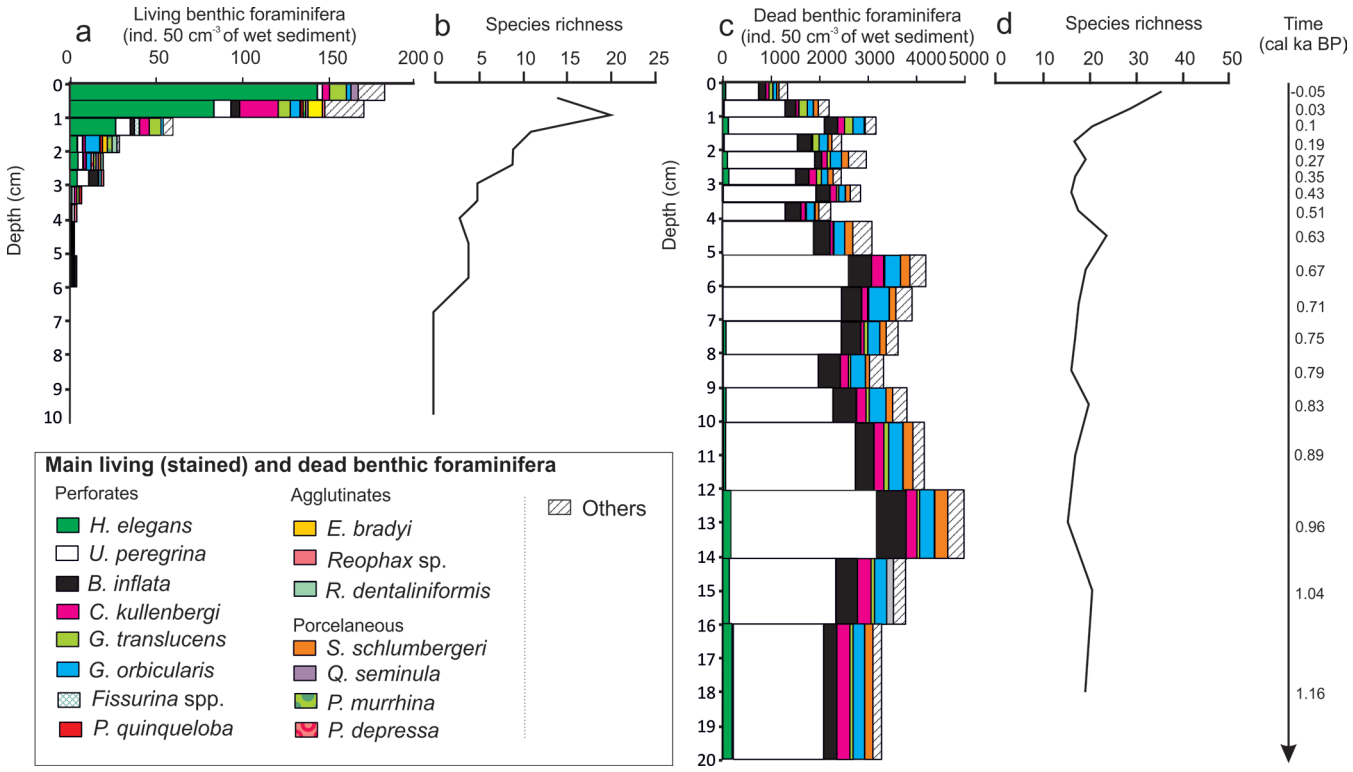

Fig. 3. Benthic foraminiferal fauna characteristics of Core FC WH: **a** – densities of the main (> 5% in at least one sample) living benthic foraminifera (ind. 50 cm^{-3} of wet sediment); **b** – species richness of the living benthic fauna; **c** – densities of the main (> 5% in at least one sample) dead benthic foraminiferal species (ind. 50 cm^{-3} of wet sediment); **d** – species richness of the dead benthic fauna.

Table 2. Percentages of the main foraminiferal species (present with ≥ 5% in at least one sample) and foraminiferal densities for Cores FCWH and CADIAC WH. The dead-fossil foraminiferal percentages are calculated after removing the non-fossilizing taxa. Sediment depths for Core CADIAC WH are corrected for the 4 cm surface sediment loss. Sedimentation rates, ages, sediment volumes, porosities and estimated dry sediment weights are indicated.

									Major benthic species																		Major planktic species											
										Perforates										Porcelanaeous				Agglutinates														
		Sedimentation rates	Sediment depth	Age	Sampled volume	Porosity	Estimated dry sediment weight	Split	*Bulimina inflata*	*Cassidulina carinata*	*Cibicidoides kullenbergi*	*Fissurina spp.*	*Gavelinopsis translucens*	*Globobulimina affinis*	*Gyroidina orbicularis*	*Hoeglundina elegans*	*Nonionella sp.*	*Uvigerina peregrina*	*Pyrgo depressa*	*Pyrgo murrhina*	*Quinqueloculina seminula*	*Sigmoilopsis schlumbergeri*	*Eggerella bradyi*	*Reophax dentaliniformis*	*Reophax sp.*	Number of picked foraminifera	Total estimated	Total estimated minus non fossilising agglutinates	Split	*Globigerina bulloides*	*Globigerinita glutinata*	*Globigerinoides ruber*	*Neogloboquadrina incompta*	*Neogloboquadrina pachyderma s.*	*Globorotalia inflata*	*Globorotalia scitula*	*Orbulina universa*	*Turborotalia quinqueloba*	Number of picked foraminifera	Total estimated
		cm³ ka⁻¹	cm	cal ka BP	cm³	–	g	–	%	%	%	%	%	%	%	%	%	%	%	%	%	%	%	%	Ind	Ind	Ind	–	%	%	%	%	%	%	%	%	%	Ind	Ind
Core FCWH	Living foraminifera	–	0.25	–	36.00	0.86	13.50	1.00	0.00	–	2.30	0.00	5.30	0.00	1.50	78.60	0.00	1.50	0.00	0.00	2.30	0.00	0.00	0.00	0.00	131	–	125	–	–	–	–	–	–	–	–	–	–	–	–
		–	0.75	–	36.00	0.83	15.80	1.00	3.28	–	13.10	0.00	4.10	0.00	3.30	49.20	0.00	5.70	0.00	0.80	0.80	0.00	4.90	0.00	0.80	122	–	116	–	–	–	–	–	–	–	–	–	–	–	–
		–	1.25	–	36.00	0.81	17.70	1.00	4.65	–	9.30	0.00	11.60	0.00	0.00	44.20	0.00	14.00	0.00	0.00	0.00	0.00	2.30	0.00	0.00	43	–	40	–	–	–	–	–	–	–	–	–	–	–	–
		–	1.75	–	36.00	0.80	19.40	1.00	0.00	–	5.00	0.00	0.00	0.00	30.00	15.00	0.00	10.00	0.00	10.00	0.00	0.00	10.00	10.00	0.00	20	–	17	–	–	–	–	–	–	–	–	–	–	–	–
		–	2.25	–	36.00	0.78	20.70	1.00	0.00	–	7.10	0.00	0.00	0.00	14.30	28.60	0.00	14.30	7.10	7.10	7.10	7.14	0.00	0.00	0.00	14	–	13	–	–	–	–	–	–	–	–	–	–	–	–
		–	2.75	–	36.00	0.77	21.80	1.00	28.57	–	0.00	0.00	0.00	0.00	35.70	21.40	0.00	7.10	0.00	0.00	0.00	0.00	0.00	0.00	7.10	14	–	13	–	–	–	–	–	–	–	–	–	–	–	–
		–	3.25	–	36.00	0.76	22.70	1.00	0.00	–	20.00	0.00	20.00	0.00	0.00	20.00	0.00	20.00	0.00	0.00	0.00	0.00	0.00	0.00	0.00	5	–	5	–	–	–	–	–	–	–	–	–	–	–	–
		–	3.75	–	36.00	0.75	23.50	1.00	0.00	–	0.00	0.00	0.00	0.00	0.00	33.30	0.00	0.00	0.00	0.00	0.00	0.00	0.00	0.00	33.30	3	–	2	–	–	–	–	–	–	–	–	–	–	–	–
		–	4.50	–	72.00	0.74	48.80	1.00	0.00	–	25.00	25.00	25.00	0.00	0.00	0.00	0.00	16.70	0.00	0.00	0.00	0.00	0.00	0.00	0.00	4	–	4	–	–	–	–	–	–	–	–	–	–	–	–
		–	5.50	–	72.00	0.73	50.50	1.00	0.00	–	33.30	0.00	0.00	0.00	16.70	0.00	0.00	0.00	0.00	0.00	0.00	0.00	0.00	0.00	0.00	6	–	6	–	–	–	–	–	–	–	–	–	–	–	–
		–	6.50	–	72.00	0.73	52.50	1.00	0.00	–	0.00	0.00	0.00	0.00	0.00	0.00	0.00	0.00	0.00	0.00	0.00	0.00	0.00	0.00	0.00	0	–	0	–	–	–	–	–	–	–	–	–	–	–	–
		–	7.50	–	72.00	0.72	54.20	1.00	0.00	–	0.00	0.00	0.00	0.00	0.00	0.00	0.00	0.00	0.00	0.00	0.00	0.00	0.00	0.00	0.00	0	–	0	–	–	–	–	–	–	–	–	–	–	–	–
		–	8.50	–	72.00	0.71	56.30	1.00	0.00	–	0.00	0.00	0.00	0.00	0.00	0.00	0.00	0.00	0.00	0.00	0.00	0.00	0.00	0.00	0.00	0	–	0	–	–	–	–	–	–	–	–	–	–	–	–
		–	9.50	–	72.00	0.69	58.60	1.00	0.00	–	0.00	0.00	0.00	0.00	0.00	0.00	0.00	0.00	0.00	0.00	0.00	0.00	0.00	0.00	0.00	0	–	0	–	–	–	–	–	–	–	–	–	–	–	–
	Dead foraminifera	6.23	0.25	−0.046	36.00	0.86	13.50	2.00	12.14	0.44	5.30	–	6.20	0.00	6.40	3.80	0.00	53.90	0.00	0.70	0.00	3.75	0.40	–	–	484	968	906	16	22.15	3.69	0.31	43.08	0.62	17.54	2.15	6.46	2.46	325	5,200
		6.23	0.75	0.03	36.00	0.83	15.80	8.00	11.05	0.53	2.60	–	8.40	0.00	5.80	1.60	0.00	59.50	0.00	0.00	0.00	4.74	1.10	–	–	199	1,592	1,520	32	22.39	2.76	2.15	41.10	0.00	16.87	4.91	4.91	0.61	326	10,432
		6.23	1.25	0.11	36.00	0.81	17.70	8.00	9.06	0.00	4.70	–	5.80	0.00	7.60	3.60	0.00	64.50	0.00	0.00	0.00	0.72	0.00	–	–	287	2,296	2,208	32	25.89	1.62	1.94	47.25	0.32	13.59	2.91	2.59	2.27	309	9,888
		6.23	1.75	0.20	36.00	0.80	19.40	8.00	11.93	0.46	0.90	–	5.50	0.00	7.30	1.40	0.00	62.40	0.00	0.00	0.00	3.21	1.80	–	–	223	1,784	1,744	32	22.99	1.49	0.90	54.03	0.00	13.43	1.79	1.49	2.09	335	10,720
		6.23	2.25	0.28	36.00	0.78	20.70	8.00	5.16	1.59	4.00	–	2.40	0.00	8.30	3.60	0.00	64.30	0.00	0.00	0.00	5.16	0.00	–	–	269	2,152	2,016	32	13.10	4.15	0.96	53.67	0.32	20.77	2.56	1.60	0.64	313	10,016
		6.23	2.75	0.36	36.00	0.77	21.80	8.00	11.52	0.00	6.50	–	4.10	0.00	5.50	5.50	0.00	57.10	0.00	0.00	0.00	4.61	0.50	–	–	225	1,8	1,736	8	15.06	4.69	1.73	51.36	0.00	22.22	0.74	2.22	0.49	405	3,240
		6.23	3.25	0.44	36.00	0.76	22.70	8.00	10.76	0.00	4.80	–	1.60	0.00	4.80	0.80	0.00	68.50	0.00	0.00	0.00	3.59	0.80	–	–	260	2,08	2,008	8	14.83	0.38	0.38	47.15	0.00	29.66	1.14	3.04	0.00	263	2,104
		6.23	3.75	0.52	36.00	0.75	23.50	8.00	15.43	0.00	4.30	–	1.10	0.00	8.00	0.00	0.00	61.70	0.00	0.00	0.00	3.72	1.10	–	–	202	1,616	1,504	8	17.35	0.00	1.83	52.97	0.00	24.66	0.46	1.83	0.00	219	1,752
		25.96	4.50	0.64	72.00	0.74	48.80	8.00	11.97	0.39	2.10	–	0.40	0.00	7.70	0.60	0.00	64.90	0.00	0.00	0.00	5.79	0.40	–	–	557	4,456	4,144	64	13.01	0.41	1.63	57.32	0.00	23.17	0.41	1.63	0.41	246	15,744
		25.96	5.50	0.68	72.00	0.73	50.50	8.00	11.82	0.41	6.10	–	0.50	0.00	8.00	0.30	0.00	63.00	0.00	0.00	0.00	4.76	0.70	–	–	766	6,128	5,888	16	8.24	1.30	1.74	61.61	1.08	19.52	0.87	2.82	0.00	461	7,376
		25.96	6.50	0.71	72.00	0.73	52.50	16.00	11.05	0.29	3.20	–	0.60	0.00	11.00	0.00	0.00	64.00	0.00	0.00	0.00	3.49	1.20	–	–	354	5,664	5,504	8	7.03	1.52	0.19	59.13	0.00	24.14	0.00	5.70	0.19	526	4,208
		25.96	7.50	0.75	72.00	0.72	54.20	16.00	11.18	0.31	1.90	–	2.20	0.00	7.10	1.60	0.00	66.50	0.00	0.30	0.00	3.73	0.60	–	–	328	5,248	5,152	32	9.92	1.07	1.74	63.94	0.67	17.02	0.00	2.28	0.27	746	23,872
		25.96	8.50	0.79	72.00	0.71	56.30	8.00	14.12	0.17	5.00	–	1.30	0.00	9.20	0.00	0.00	59.30	0.00	0.00	0.00	2.52	0.70	–	–	602	4,816	4,760	16	10.69	2.20	1.57	60.06	0.31	20.13	0.00	3.62	0.63	636	10,176
		25.96	9.50	0.83	72.00	0.69	58.60	8.00	12.85	0.29	5.10	–	1.80	0.00	9.20	1.50	0.00	58.00	0.00	0.10	0.00	3.65	1.30	–	–	689	5,512	5,480	32	9.18	1.90	1.31	60.35	0.15	19.83	0.15	3.64	0.58	686	21,952
		25.96	11.00	0.89	144.00	0.70	115.50	32.00	9.36	0.00	4.80	–	2.40	0.00	7.00	1.10	0.00	64.20	0.00	0.50	0.00	4.81	0.80	–	–	374	11,968	11,968	64	12.22	2.36	1.94	54.86	0.14	19.03	0.56	4.44	0.56	720	46,080
		25.96	13.00	0.96	144.00	0.65	133.00	32.00	12.58	0.00	4.40	–	1.10	0.00	6.00	3.30	0.00	59.40	0.00	0.00	0.00	5.30	0.40	–	–	453	14,496	14,496	64	15.00	3.13	1.56	49.06	0.31	21.25	0.94	5.94	0.31	320	20,480
		25.96	15.00	1.04	144.00	0.59	157.80	16.00	11.89	0.29	7.30	–	1.90	0.00	6.60	3.50	0.00	57.90	0.00	0.60	0.10	3.67	0.90	–	–	681	10,896	10,896	32	14.89	3.10	2.85	43.67	0.87	17.87	0.50	12.28	1.12	806	25,792
		25.96	18.00	1.16	288.00	0.63	283.00	64.00	9.46	0.34	8.10	–	2.00	0.00	7.10	5.70	0.00	56.40	0.30	0.70	0.00	5.07	1.00	–	–	296	18,944	18,944	128	16.39	4.84	3.96	45.87	0.33	14.30	2.31	7.70	0.77	909	116,352

									Major benthic species																		Major planktic species										
									Perforates										Porcelanaeous				Agglutinates															
		Sedimentation rates	Sediment depth	Age	Sampled volume	Porosity	Estimated dry sediment weight	Split	*Bulimina inflata*	*Cassidulina carinata*	*Cibicidoides kullenbergi*	*Fissurina spp.*	*Gavelinopsis translucens*	*Globobulimina affinis*	*Gyroidina orbicularis*	*Hoeglundina elegans*	*Nonionella sp.*	*Uvigerina peregrina*	*Pyrgo depressa*	*Pyrgo murrhina*	*Quinqueloculina seminula*	*Sigmoilopsis schlumbergeri*	*Eggerella bradyi*	*Reophax dentaliniformis*	*Reophax sp.*	Number of picked foraminifera	Total estimated	Total estimated minus non fossilising agglutinates	Split	*Globigerina bulloides*	*Globigerinita glutinata*	*Globigerinoides ruber*	*Neogloboquadrina incompta*	*Neogloboquadrina pachyderma s.*	*Globorotalia inflata*	*Globorotalia scitula*	*Orbulina universa*	*Turborotalia quinqueloba*	Number of picked foraminifera	Total estimated
		$cm^3 ka^{-1}$	cm	cal ka BP	cm^3	–	g	–	%	%	%	%	%	%	%	%	%	%	%	%	%	%	%	%	Ind	Ind	Ind	–	%	%	%	%	%	%	%	%	%	Ind	Ind
Core CADIAC WH	Fossile foraminifera	6.23	4.50	0.64	35.42	0.79	19.40	4.00	12.26	0.77	4.60	–	0.40	0.00	6.90	1.10	0.00	63.20	0.00	0.00	0.00	2.30	0.80	–	–	285	1,14	1,044	16,00	5.91	1.18	1.18	66.43	0.24	17.02	0.00	2.84	0.00	423	6,768
		25.96	9.50	0.83	35.42	0.76	22.10	4.00	13.56	0.56	5.10	–	2.50	4.20	3.70	3.10	0.00	52.50	0.00	1.10	0.00	3.95	2.30	–	–	364	1,456	1,416	16	1.74	1.45	2.33	69.04	0.73	15.12	0.00	3.78	0.00	688	11,008
		25.96	14.50	1.02	35.42	0.74	24.30	4.00	11.96	0.36	2.50	–	2.90	0.40	4.70	5.80	0.00	57.20	0.00	0.40	0.00	3.99	1.10	–	–	286	1,144	1,104	32	14.55	1.82	2.18	58.55	0.18	13.45	1.09	4.00	0.73	550	17,600
		27.98	19.50	1.21	35.42	0.72	26.10	4.00	16.60	1.93	6.20	–	2.70	1.20	6.90	3.50	0.00	44.80	0.00	0.40	0.00	3.09	1.90	–	–	260	1,04	1,036	32	15.65	1.59	2.92	48.28	0.80	19.63	0.53	5.31	0.27	377	12,064
		27.98	24.50	1.39	35.42	0.71	27.50	4.00	13.89	0.69	4.20	–	7.60	1.60	4.90	4.40	0.00	44.20	0.00	0.20	0.90	3.47	1.40	–	–	437	1,748	1,728	32	13.81	3.50	4.28	52.14	0.58	12.45	0.97	4.47	1.36	514	16,448
		27.98	29.50	1.57	35.42	0.69	28.70	8.00	13.46	0.38	5.00	–	6.90	1.50	3.80	4.20	0.00	50.00	0.00	0.40	0.40	3.46	1.90	–	–	262	2,096	2,080	32	15.65	3.55	3.55	50.65	0.00	12.42	2.58	3.06	0.65	620	19,840
		27.98	34.50	1.75	35.42	0.68	29.70	4.00	9.86	0.28	6.50	–	5.60	1.10	3.70	2.80	0.00	58.00	0.00	1.10	0.60	3.10	0.60	–	–	355	1,42	1,420	32	13.51	2.14	6.10	49.92	1.32	12.19	0.66	6.75	0.99	607	19,424
		27.98	39.50	1.92	35.42	0.67	30.50	4.00	10.86	1.04	4.00	–	6.70	1.30	6.10	5.80	0.00	46.80	0.00	2.90	0.20	4.18	1.50	–	–	479	1,916	1,916	32	13.16	3.34	4.72	54.03	0.39	9.23	2.55	2.75	0.98	509	16,288
		27.98	44.50	2.10	35.42	0.67	31.30	4.00	12.66	0.76	6.30	–	5.30	1.00	4.60	3.30	0.00	54.70	0.00	0.30	0.30	3.29	1.50	–	–	395	1,58	1,580	32	12.36	2.39	6.29	56.18	0.87	4.99	0.87	8.46	0.43	461	14,752
		27.98	49.50	2.28	35.42	0.66	31.90	4.00	9.65	1.16	4.80	–	9.70	0.60	5.40	7.50	0.00	47.50	0.00	0.80	0.60	2.32	1.70	–	–	518	2,072	2,072	64	14.88	1.73	9.34	51.56	1.04	7.61	1.04	3.46	1.73	289	18,496
		27.98	54.50	2.46	35.42	0.65	32.40	4.00	10.69	1.27	5.60	–	3.80	0.00	8.90	2.50	0.00	53.90	0.00	0.80	0.00	1.02	0.80	–	–	393	1,572	1,572	32	11.44	1.78	9.47	56.02	0.39	7.30	0.20	5.92	0.00	507	16,224
		27.98	59.50	2.64	35.42	0.65	32.90	8.00	10.36	0.71	5.00	–	5.70	1.10	7.50	3.60	0.00	54.60	0.00	1.10	0.40	2.14	0.40	–	–	280	2,24	2,240	64	9.76	3.17	4.22	63.59	0.79	3.69	0.79	6.60	1.06	379	24,256
		4.61	64.50	3.72	35.42	0.64	33.30	8.00	7.81	1.56	4.10	–	5.00	0.00	5.90	5.90	0.00	53.80	0.00	2.20	0.30	3.44	2.20	–	–	320	2,56	2,560	64	13.59	2.99	2.72	55.16	0.54	2.99	1.36	9.78	0.54	368	23,552
		4.61	69.50	4.81	35.42	0.64	33.70	8.00	8.72	0.62	6.90	–	8.40	0.90	8.10	3.70	0.00	47.70	0.00	1.60	0.30	2.18	2.50	–	–	321	2,568	2,568	64	12.90	3.81	3.52	53.37	0.00	3.23	0.59	11.14	1.47	341	21,824
		4.61	74.50	5.89	35.42	0.64	34.10	8.00	9.09	1.52	8.80	–	9.10	2.10	6.40	4.80	0.00	45.50	1.20	0.30	0.00	3.94	2.10	–	–	331	2,648	2,640	64	7.78	8.33	4.17	50.00	0.56	6.67	1.11	8.33	0.28	360	23,040
		1.16	76.50	7.62	35.42	0.63	34.30	8.00	9.38	2.05	3.80	–	12.60	0.00	7.30	5.00	0.30	45.20	0.00	0.90	0.30	2.35	1.50	–	–	341	2,728	2,728	64	12.47	5.54	3.23	43.42	3.00	10.16	1.15	7.39	1.85	433	27,712
		1.16	77.50	8.49	35.42	0.63	34.40	8.00	17.97	3.39	7.80	–	13.90	1.40	5.10	6.10	0.70	25.40	0.00	2.00	1.00	3.39	2.70	–	–	298	2,384	2,360	64	9.05	7.33	3.45	46.98	1.94	9.48	1.51	9.48	0.65	464	29,696
		1.16	79.50	10.22	35.42	0.63	34.50	4.00	20.73	5.70	11.10	–	15.50	0.00	3.60	6.20	0.00	4.90	0.50	3.90	0.30	7.77	2.60	–	–	388	1,552	1,544	64	13.75	7.67	6.08	37.34	1.59	16.64	0.87	4.63	2.75	691	44,224
		1.92	81.50	11.26	35.42	0.63	34.70	4.00	24.31	4.13	6.00	–	11.50	3.70	4.10	5.00	3.20	4.10	0.00	0.90	0.90	4.59	6.00	–	–	221	884	872	64	17.26	7.90	4.16	24.74	20.17	7.90	1.04	1.46	9.15	481	30,784
		1.92	84.50	12.82	35.42	0.63	34.90	4.00	19.09	4.09	1.80	–	10.00	6.40	0.00	0.90	14.10	0.90	0.90	8.60	0.50	3.18	5.50	–	–	220	880	880	64	17.06	11.11	8.73	30.95	8.33	9.52	1.19	0.79	5.16	252	16,128

of the dead benthic fauna generally increase down core (min = 1,340 ind. 50 cm^{-3} at 0–0.5 cm; max = 5,030 ind. 50 cm^{-3} at 12–14 cm). The dead benthic fauna is largely dominated by *U. peregrina* (59.7%). The other common species were *B. inflata* (11.0%), *G. orbicularis* (7.2%), *C. kullenbergi* (5.2%), *S. schlumbergeri* (4.3%), *H. elegans* (2.5%), and *G. translucens* (1.9%) (Fig. 3c; Table 2). The species richness rapidly descends down core, from 36 in the surficial layer to about 20 in the lower part of the core (Fig. 3d). This is mainly due to a progressive disappearance of non-fossilizing agglutinants.

When comparing the living fauna with the average dead assemblage and after removing the non-fossilizing taxa, *H. elegans, C. kullenbergi,* and *G. translucens* have a higher percentage in the living than in the dead assemblage ($0.5 < L/(L + D) < 1.0$) (Table 3). Conversely, *U. peregrina, B. inflata* and *S. schlumbergeri* present a higher percentage in the dead than in living assemblages ($0 < L/(L + D) < 0.5$). *Gyroidina orbicularis* shows a relatively balanced pattern between living and dead assemblages ($L/(L + D) = 0.44$).

Fossil faunas

Foraminiferal concentrations and accumulation rates

For each sub-sample of the 20 cm long Core FC WH, absolute abundances of living and dead benthic foraminifera are summed up and expressed in ind. g^{-1} of dry sediment, to be comparable to the 85 cm long Core CADIAC WH (Fig. 4a). Non-fossilizing agglutinated taxa have been excluded from the dataset beforehand. Only *Eggerella bradyi*, *Karreriella bradyi* and *Textularia* spp. are considered as fossilizing agglutinated taxa because of their continuous presence down core. Consequently, the total abundance of benthic fauna for the two stacked Cores FC WH and CADIAC WH (without non-fossilizing species) varies between a minimum of 25 ind. g^{-1} at ~ 11.2 cal ka BP and a maximum of 125 ind. g^{-1} at ~ 0.1cal ka BP (Fig. 4a). Absolute densities of planktic foraminifera vary between 75 ind. g^{-1} at 0.5 cal ka BP and 1,280 ind. g^{-1} around 10.2 cal ka BP (Fig. 4b). Throughout the record, BFARs are well correlated to PFARs (Fig. 4). BFARs and PFARs range from ~ 130 ind. cm^{-2} ka^{-1} (11.2 cal ka BP) to 7,900 ind. cm^{-2} ka^{-1} (0.6 cal ka BP) and from ~ 1,230 ind. cm^{-2} ka^{-1} (0.5 cal ka BP) to 54,700 ind. cm^{-2} ka^{-1} (2.6 cal ka BP), respectively. Both BFARs and PFARs are low from 12.8 to 3.5 cal ka BP and after 0.6 cal ka BP, whereas maxima are observed between 3.5 and 0.6 ka BP in a period of high sedimentation rates (Fig. 2).

Foraminiferal assemblages in Core CADIAC WH

A total of 89 benthic species are identified in the record of the 85 cm long Core CADIAC WH. The main benthic species are *Uvigerina peregrina*, *Bulimina inflata*, *Gyroidina orbicularis*, *Cibicidoides kullenbergi*, *Gavelinopsis translucens*, *Sigmoilopsis schlumbergeri*, *Hoeglundina elegans*, *Eggerella bradyi*, C*assidulina carinata*, *Pyrgo murrhina*, *Globobulimina affinis*, and *Nonionella* sp. (Fig. 4a; Table 2). A first group of benthic species (*E. bradyi*, *P. murrhina, G. affinis*, and *Nonionella* sp.) shows the highest relative frequencies in the lowest part of the core, followed by a rapid decrease to ≤ 3% at ~ 10.2 cal ka BP. A second group of benthic species (*B. inflata*, *G. translucens*, *C. kullenbergi*, *S. schlumbergeri*, *C. carinata*, and *H. elegans*) shows maximum abundances around 10.2 cal ka BP; thereafter, they progressively decrease until ~ 7.6 cal ka BP. The relative abundance pattern of *U. peregrina* can be subdivided into three parts: it is infrequent from 12.8 to 10.2 cal ka BP, rapidly increases from 10.2 to 7.6 cal ka BP (up to ~ 45%), and becomes dominant in the last ~ 7.9 cal ka BP where it accounts for ~ 50% of the faunas. Maximum percentages (63%) are observed towards the top of the core (Fig. 4a). During the last 7.9 ka BP, other common species are *B. inflata*, *G. or-*

Table 3. Ratio L/(L + D) (Living/(Living + Dead)) for the 6 main fossilizing benthic species calculated for the total living and dead fossilizing foraminiferal densities from Core FC WH; in bold, values between 0.5 and 1.0 (higher % in living fauna), and in black boxes values between 0.0 and 0.5 (higher % in dead fauna).

Species	*H. elegans*	*C. kullenbergi*	*U. peregrina*	*G. orbicularis*	*G. translucens*	*B. inflata*	*S. schlumbergeri*
% Living (L)	57.77	8.5	6.74	5.87	5.57	2.93	0.29
% Dead (D)	1.93	4.8	60.99	7.58	2.28	11.6	4.04
L/(L + D)	**0.97**	**0.64**	**0.1**	0.44	**0.71**	0.2	0.07

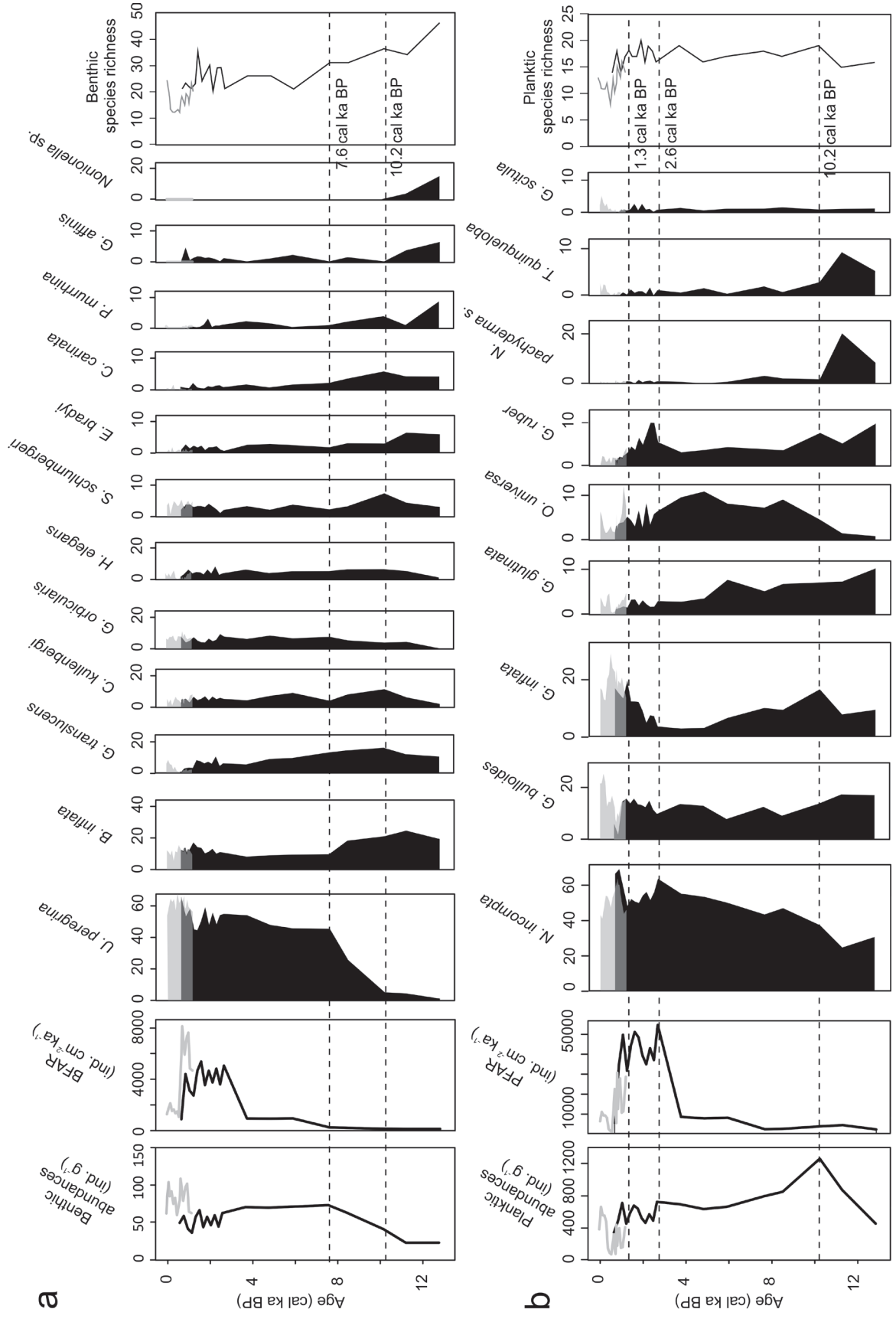

Fig. 4. a – time records in Cores CADIAC WH (black color) and FC WH (grey color) of benthic foraminiferal abundances (ind. g^{-1} of dry sediment), benthic foraminiferal accumulation rates (ind. cm^{-2} ka^{-1}), relative abundances of the main benthic species present with ≥ 5% in at least one sample (after removing the non-fossilizing taxa), and species richness; **b** – time records in Cores CADIAC WH (black color) and FC WH (grey color) of planktic foraminiferal abundances (ind. g^{-1} of dry sediment), same indications as for benthic faunas. The horizontal dotted lines delimitate the major foraminiferal changes (see text for all the details).

bicularis, *C. kullenbergi*, and *S. schlumbergeri*, all with rather stable percentages. *Hoeglundina elegans* and *G. translucens* show a decrease in the last 2,000 years. The taxa *E. bradyi*, *C. carinata*, *G. affinis*, *P. murrhina* and *Nonionella* sp. almost disappear in the upper part of the record. Benthic species richness decreases progressively towards the top of the core with a distinct minimum of 12 species at 0.3 cal ka BP (Fig. 4a).

A total of 23 planktic species are identified. The main planktic species observed are *Neogloboquadrina incompta*, *Globorotalia inflata*, *Globigerina bulloides*, *Orbulina universa*, *Globigerinita glutinata*, *Globigerinoides ruber* (white), *Neogloboquadrina pachyderma sinistral*, *Turborotalia quinqueloba* and *Globorotalia scitula* (Fig. 4b; Table 2). *Turborotalia quinqueloba* and *N. pachyderma* s. show maximum abundances in the basal part of the core (~ 11.2 cal ka BP; 9.0 and 20.0%, respectively) and become less frequent after 10.2 cal ka BP. *Neogloboquadrina incompta* progressively increases from ~ 30.0% at 12.8 ka BP, to ~ 60.0% at the core top, whereas *G. glutinata* shows a general decrease from ~ 10.0 to 1.0%. *Globigerina bulloides* remains present with 10–15%, except around 0.8 cal ka BP where it suddenly drops to 1.7% and during the last 0.2 cal ka BP when it attains ~ 20.0%. High relative abundances of *O. universa* are observed from 10.2 to 2.6 cal ka BP, whereas *G. ruber* is more abundant from 12.8 to 10.2 cal ka BP and from 2.6 to 2.0 cal ka BP. *Globorotalia inflata* is dominant in the early record, decreases to reach minimal values (~ 3.3%) around 3.7 cal ka BP, and increases again towards the top of the core (~ 30%). Planktic species richness is rather stable, but decreases progressively during the last 2,000 years, with a distinct minimum of 8 species at 0.5 cal ka BP (Fig. 4b).

Stable isotope analyses

Stable oxygen and carbon isotope ratios ($\delta^{18}O$ and $\delta^{13}C$) are more positive in *Globorotalia inflata* than in *Globigerina bulloides* (Fig. 5). The $\delta^{18}O$ of both species is high at 12.8–11.2 cal ka BP, and then decreases until 8.5 cal ka BP. Relatively stable values (about + 0.55‰ for *G. bulloides*, and + 1.00‰ for *G. infla-*

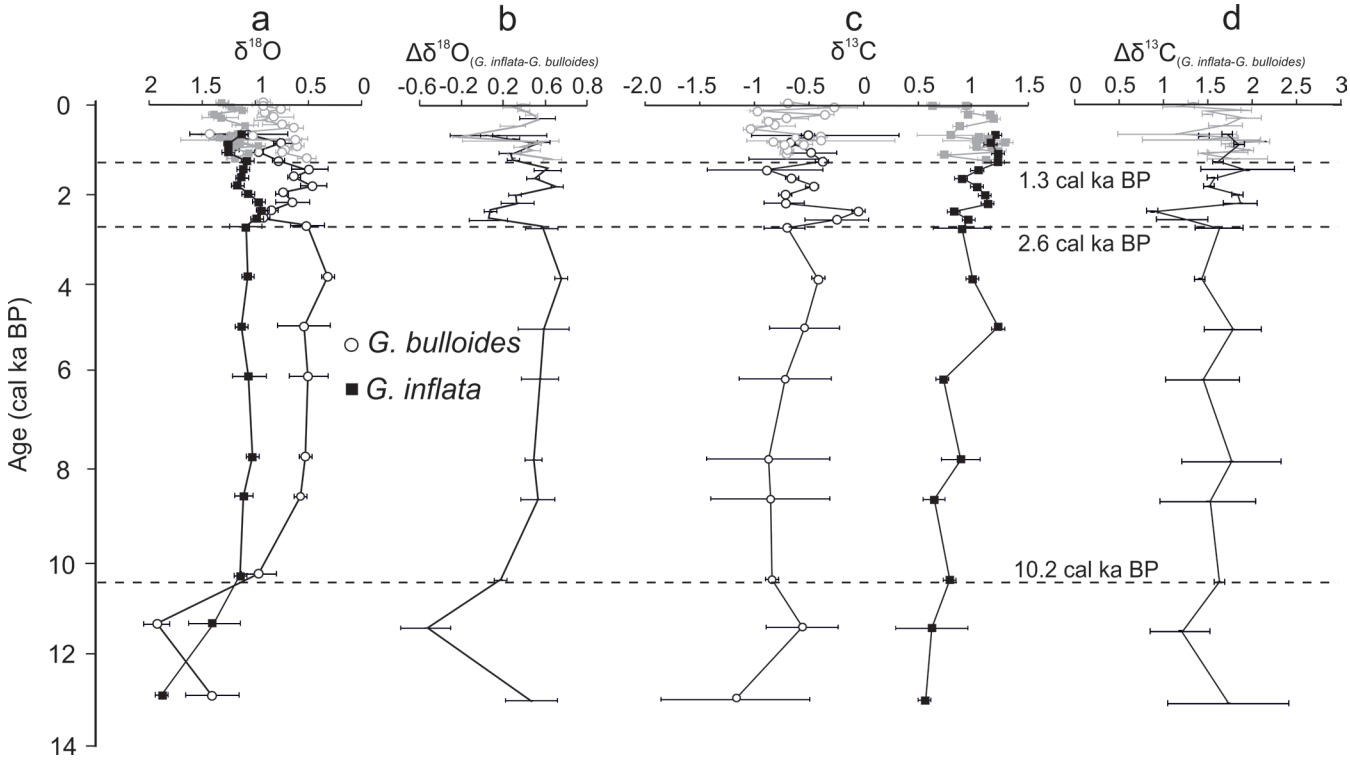

Fig. 5. a – oxygen stable isotope ratios ($\delta^{18}O$) performed on *G. bulloide*s and *G. inflata*; **b** – $\Delta\delta^{18}O$ between $\delta^{18}O_{G.\ inflata}$ and $\delta^{18}O_{G.\ bulloides}$; c – carbon stable isotope ratios ($\delta^{13}C$) performed on *G. bulloide*s and *G. inflata*; **d** – $\Delta\delta^{13}C$ between $\delta^{13}C_{G.\ inflata}$ and $\delta^{13}C_{G.\ bulloides}$. The grey lines represent FC WH and the black colour represents CADIAC WH. The horizontal dotted lines delimitate the major changes (see text for all the details).

ta) are observed until ~ 2.6 cal ka BP. From then on, *G. bulloides* shows an increasing trend towards the top of the record, interrupted by a short event of maximum $\delta^{18}O_{G.\ bulloides}$ values (0.97‰) at ~ 2.4 cal ka BP. A similar, but much weaker trend to more positive values can be seen for *G. inflata*. The difference between the two oxygen ratios ($\Delta\delta^{18}O = \delta^{18}O_{G.\ inflata} - \delta^{18}O_{G.\ bulloides}$) fluctuates around 0.5‰, but shows some remarkable events around 2.3 and 0.7 cal ka BP when the $\Delta\delta^{18}O$ is close to zero. $\delta^{13}C_{G.\ bulloides}$ varies between –1.17‰ and –0.05‰, whereas $\delta^{13}C_{G.\ inflata}$ ranges from 0.56‰ to 1.25‰. The $\delta^{13}C$ of both species increases from 12.8 to ~ 4.8 cal ka BP and then fluctuates around –0.55‰ for *G. bulloides* and 1.1‰ for *G. inflata*. Around 2.3 cal ka BP, $\delta^{13}C_{G.\ bulloides}$ shows heavier values. The $\Delta\delta^{13}C = \delta^{13}C_{G.\ inflata} - \delta^{13}C_{G.\ bulloides}$ remains fairly constant over the record (~ 1.65‰), and only decreases around 2.4 cal ka BP to ~ 1.00‰.

DISCUSSION

Living (stained) benthic foraminiferal assemblages

Regarding the large existing data set on living benthic assemblages collected in the BoB in different seasons and at several water depths (see review in Mojtahid *et al.* 2010), complemented by the present study, we dispose of a very good knowledge of the primary ecological parameters controlling the variability of the dominant benthic species. This knowledge will largely contribute to the reliability of the paleoceanographic interpretations of sediment archives from the BoB, among which our 2,000 m deep Station WH.

At Station WH, living benthic foraminifera mainly occupy the top centimeter of the sediment resulting in an average living depth of 1.02 cm (Fig. 3). The rather low estimated organic matter fluxes (3.2 g C m^{-2} yr^{-1}) are responsible for the rather deep oxygen penetration (5 cm) into the sediment (Fontanier *et al.* 2002, Mouret *et al.* 2010) and the shallow foraminiferal microhabitats at Station WH (TROX model; Jorissen *et al.* 1995). It appears that the 2,000 m deep Station WH is located today in a realm with oligotrophic baseline conditions.

The composition of our living benthic foraminiferal faunas can be compared with the results of an earlier ecological study on an interface core sampled in October 1997 at the same location (Fontanier *et al.* 2002). The benthic foraminiferal standing stocks are two times higher in June 2006 (~ 250 ind. 50 cm^{-2}) than in October 1997 (~ 125 ind. 50 cm^{-2}). The higher densities in June 2006 could be explained by a period of higher benthic production in response to enhanced fresh organic matter input resulting from an unusually intense late spring bloom (Retailleau *et al*. 2009, Kuhnt *et al*. 2013). It appears therefore that at this 2,000 m deep environment in the BoB, substantial seasonal pulses of labile organic matter input are superposed on the oligotrophic baseline conditions. These dual characteristics may explain the strong dominance throughout the year of the rather oligotrophic species *Hoeglundina elegans*, which represents about 34.9% of the total living fauna in October 1997 (Fontanier *et al.* 2002) and about 54.4% in June 2006 (this study). The discrepancy between oligotrophic baseline conditions and short periods of enhanced organic matter input may also explain the large fluctuations in the relative abundances of *U. peregrina* at our 2,000 m site, from ~ 25% in October 1997 (Fontanier *et al.* 2002) to only 6.4% in June 2006 (this study). *Uvigerina peregrina* is considered as an opportunistic species, being the first large-sized (> 150 µm) species to respond to phytoplankton blooms occurring in the area (Fontanier *et al.* 2002), and could be favored by diatom-rich phytodetritus (Goldstein and Corliss 1994). Phytoplankton assemblages in the BoB change on a seasonal scale (e.g. Lampert 2001). Coccolithophores are present through the year and may exhibit a large bloom in summer, triggered by sporadic upwellings (e.g. Beaufort and Heussner 1999). Diatoms exhibit a strong seasonal variation with high abundances during spring bloom and significant secondary peaks in winter, profiting from riverine nutrient input in the BoB (e.g. Beaufort and Heussner 1999). The very late intense phytoplankton bloom of June 2006, potentially dominated by coccolithophores, apparently has favored the dominant species *H. elegans*, and not *U. peregrina*. High relative abundances of *U. peregrina* in October 1997 (and in the early spring bloom observed at other stations, see Fontanier *et al.* 2003, 2005) in the BoB corroborates the putative ecological dependence of this species on phytodetritus dominated by diatom remains.

Comparison of living and dead/fossil assemblages in Core FC WH

When comparing the living benthic foraminiferal fauna to the dead assemblages at Station WH, some notable differences in species composition can be observed. These differences can be attributed to various taphonomic processes (i.e. destruction of tests) and biological factors (i.e. population dynamics) (e.g. Jorissen

and Wittling 1999, Duros *et al.* 2011). First of all, organic-walled agglutinated taxa, such as *Reophax* spp., are not preserved in the fossil assemblages (e.g. Bizon and Bizon 1984). Agglutinated species with calcareous cement (e.g. *Eggerella bradyi*) are well represented in the dead fauna. Although taphonomic processes can be of great consequence in deep-sea environments dominated by agglutinated taxa (e.g. Gooday 2003), at our 2,000 m deep site, non-fossilizing agglutinated taxa are rather subordinate, together counting for only ~ 6% of the total living fauna.

The calcareous taxa strongly dominate living as well as fossil assemblages, and it should therefore be possible to produce reliable paleoenvironmental reconstructions on the basis of the faunas preserved in sedimentary archives. Among the calcareous taxa, *Hoeglundina elegans* is remarkably poor in the fossil assemblages (2.1% on the average) in comparison to its very high relative abundance in the modern fauna (~ 54.4%). In fact, in our samples, *H. elegans* is the only species showing clear signs of dissolution (broken chambers, holes in the test, dull aspect), which may be due to its aragonitic test, which is more sensitive to dissolution processes than calcitic tests (e.g. Loubere and Gary 1990, Murray and Alve 1999, Corliss and Honjo 1981). It appears therefore that the under-representation of this species in the fossil fauna is the result of major taphonomical losses.

However, also several other calcareous taxa show important differences between their relative abundance in the dead fauna compared to the living assemblage (Table 3). Such discrepancies, apparently unrelated to taphonomical processes, have been frequently noted in studies comparing living and dead assemblages, and they have been tentatively ascribed to population dynamics (e.g. Jorissen and Wittling 1999, Duros *et al.* 2011). Fossil faunas tend to be dominated by opportunistic taxa, which proliferate during short periods of food abundance, which may be missed by studies based on single-time samplings. The less opportunistic taxa, which represent the more oligotrophic base-line conditions, will have a lower percentage in the time-averaged fossil samples than in snapshot recent samples; mostly missing the short productive events. At our 2,000 m deep site, *Uvigerina peregrina* presents an exceptional low L/(L + D) ratio (Table 3) with a relative frequency of 6.4% (this study) and 25% (October 1997, Fontanier *et al.* 2002) in the living fauna, compared to an average of 60% in the dead assemblages of our core. This difference can be partly explained by the poor preservation of *H. elegans,* the other dominant taxon. In fact, if we would delete *H. elegans* and all non-fossilizing agglutinants from the living faunas, *U. peregrina* would account for 16% (this study) and 44% (Fontanier *et al.* 2002). However, *U. peregrina* is also known for its strong opportunistic behavior, with a particularly high reproductive potential and turnover rate. This opportunistic behavior is probably a second reason explaining the much higher percentage in the dead/fossil faunas of Core FC WH. A high abundance of *U. peregrina* in the fossil record can therefore be interpreted as due to pulses of phytodetritus exported from highly seasonal primary production.

Summarizing, although the living assemblages cannot be used in a straightforward way as a recent analogue for fossil faunas, the sedimentary archives from the deep BoB may supply information about the dynamics of dominant foraminiferal taxa related to the pulsed input of fresh organic detritus in the benthic system. Indirectly, this could allow us to obtain information of the (paleo-) seasonality of the planktic ecosystem.

Paleoenvironmental record

Sedimentological analysis

The 12.8–7.6 cal ka BP time interval covering the YD and early Holocene is characterized by a fine laminated clay/silt facies and low sedimentation rates (~ 1.5 cm ka^{-1}). The transition from the laminated silty facies to the subsequent clayey bioturbated facies seems to be gradual (Fig. 2). Toucanne *et al.* (2008) record a similar sedimentary succession on deep-sea canyon levees of the Armorican margin of the BoB, with laminated layers of clays and silts to fine sands (~ 15.5 to 8.0 cal ka BP) underlying a homogeneous clay deposit. Such finely laminated layers are possibly deposited from the overflow of distal turbidity currents, whereas homogeneous clays are interpreted as hemipelagic deposits (Stow and Piper 1984). During the last stage of deglaciation, the BoB margin was affected by a rapid and sustained rise of the global sea-level until ~ 6–7 cal ka BP (Lambeck *et al.* 2002). This time period corresponds to the end of the laminated sedimentation events in our core, which may mark the decrease of basinward transfer of sediment by turbidity currents (Toucanne *et al.* 2008). However, sedimentation rates measured at Station WH during the laminated events are two orders of magnitude lower (~ 1.5 cm ka^{-1}) than on deep-sea canyon levees (~ 300 cm ka^{-1}) of the northern margin of the BoB (Toucanne *et al.* 2008). This may be explained by different sediment sources and the position of the sites with respect to tur-

bidite pathways. Station WH is close to the Cap Ferret Canyon system, which drained the Gironde paleoriver connected to minor glaciers of the Pyrenees; probably affecting sedimentation at Station WH. However, due to the position of Site WH on the upper left bank of the canyon and one kilometer above the channel axis, most turbidites will have bypassed this site, explaining the surprisingly low sedimentation rates. After 7.6 cal ka BP, the set up of the modern deep-sea BoB sedimentation regime is marked by the dominance of hemipelagic deposits despite its relative proximity to the Cap Ferret Canyon. Toucanne *et al.* (2008) observed a similar increase in hemipelagic sedimentation from 8 ka cal BP onward in a core from the Armorican margin of the BoB. After 7.6 cal ka BP, sedimentation rates are much higher (~ 26.9 cm ka^{-1}), especially from 2.6 to 0.6 cal ka BP. This increase in sedimentation rates may be the result of reduced current intensity due to the stabilization of sea-level (McCave *et al.* 1995) and/or an increase of sediment supplies from the Gironde fluvial plume and/or an increase of organic supply from surface water productivity.

Paleoproductivity

Foraminiferal accumulation rates (BFAR and PFAR) may be used as proxies for paleoproductivity (e.g. Herguera and Berger 1991, Jorissen *et al.* 2007). Usually, significant correlation between PFAR and BFAR is due to short term changes in sedimentation rate between age control points, but may also suggest that benthic foraminifera is closely linked to surface water production (Herguera and Berger 1991, Herguera 1992, Gooday 2003). Highest values at Station WH are observed between ~ 3.1 and 0.7 cal ka BP (Fig. 4), which correspond to the change to much higher sedimentation rates (~ 26 cm ka^{-1}) than before. This strongly suggests that higher sediment supplies coincided with a higher nutrient input into the basin, and inversely, that part of the increase in sedimentation rates may have been due to an increase in productivity. Similarly, the study of Mojtahid *et al.* (2013), performed at a 550 m deep site closer to the coast (KS10b; Fig. 1), found a high productivity period from 3.5 to 1.8 cal ka BP during an interval of stable sedimentation rates. Apparently, the ~ 3.1 and 0.7 cal ka BP interval was characterized by nutrient dispersal far into the BoB (cf. Station WH is located ~ 120 km offshore), triggering offshore phytoplankton blooms. Nutrient supplies to more offshore areas could result from intensified precipitation and subsequent increased river runoff, such as has been described at the same period along the Iberian margin (e.g. Abrantes *et al.* 2005, Bernárdez *et al.* 2008a, Pena *et al.* 2010).

Benthic assemblages

On the basis of the benthic foraminiferal succession, three main periods can be distinguished along the record (Fig. 4a):

1. The time interval from 12.8 to 10.2 cal ka BP is characterized by high abundances of species characteristic for oligotrophic environments (*Bulimina inflata*, *Eggerella bradyi,* and *Pyrgo murrhina*). The dominant fauna is mixed with high percentages of allochthonous taxa (*Nonionella* sp., *Cassidulina carinata,* and *Globobulimina affinis*, together ~ 20% of the total fauna), characteristic for eutrophic outer shelf/upper slope environments (e.g. Fontanier *et al.* 2002, 2003; Duchemin *et al.* 2007; Mojtahid *et al.* 2010). This suggests significant lateral advection of upper shelf material into an oligotrophic deep-sea environment. Subsequent decrease in abundances of the allochtonous taxa at the end of this time period indicates that downslope transport of upper shelf material was probably more pronounced and frequent process during the YD and very early Holocene. The low sea-level coupled to a narrow continental shelf may have enhanced basinward transfer of sediment by turbidity currents. Higher canyon activity is corroborated by the sedimentological characteristics of the lower part of the record until 7.6 cal ka BP: laminated layers, coarser grain size, and low sedimentation rate. Coarser grain size also characterizes this time interval at the 550 m deep Station B, located in the vicinity of the Capbreton canyon, southeastern BoB (Fig. 1; Mojtahid *et al.* 2013).

2. The beginning of the time interval from 10.2 to 7.6 cal ka BP is characterized by maximum abundances of species typical of mesotrophic to oligotrophic benthic settings in the BoB (*Gavelinopsis translucens*, *Sigmoilopsis schlumbergeri* and *Cibicidoides kullenbergi*) (Mojtahid *et al.* 2010). Next, relative abundances of *Uvigerina peregrina* sharply increase from a few % to 45%; all other species decrease in consequence, except *Gyroidina orbicularis*. This period appears as a major turnover phase for the benthic ecosystems in the Plateau des Landes, from a stable oligotrophic system to an oligotrophic system with seasonal productivity events, probably resulting from more productive surface waters. The end of this period coincides with a weakening of canyon influence and the establishment of hemipelagic sedimentation in the BoB.

3. The time interval from 7.6 cal ka BP to today is mainly characterized by the strong dominance of

U. peregrina, which suggests the establishment of contrasted seasons in the BoB area, with highly seasonal phytoplankton production (and organic fluxes to the seafloor). The shift in the climatic (summer insolation) and/or oceanographic (nutrient supply) context has provided better conditions for primary production marked by two major seasonal phytoplankton bloom periods (February–June and November–December), as observed in modern surface waters (e.g. Beaufort and Heussner 1999). The fairly stable composition of benthic assemblages, dominated by mesotrophic-eutropic species recorded after 7.6 cal ka BP testifies the long-term control of this seasonal flux regime on the benthic environment. Since a similar turnover is recorded in the SE BoB (Mojtahid *et al.* 2013), this appears to be a basin-wide development.

Planktic assemblages and stable isotope signal

In this study, two species were selected for stable isotopic measurements (*Globigerina bulloides* and *Globoratolia inflata*). The stable isotope curves of both species show a clear offset and different patterns along the record, especially for $\delta^{18}O$ (Fig. 5). These differences can be explained by their different ecological preferences and calcifying depths. *G. bulloides* is a surface dwelling species whereas *G. inflata* has a deeper habitat, as observed in the vertical distribution of the modern assemblages collected in the SE BoB (Retailleau *et al.* 2011). During the spring bloom event, *G. bulloides* mainly occupies the 0–20 m depth interval, whereas *G. inflata* peaks in the 20–40 m depth interval (Retailleau *et al.* 2011).

On the basis of planktic assemblages (Fig. 4b) and isotopic signature (Fig. 5), four main periods are recognized:

1. During the 12.8 to 10.2 cal ka BP time interval, the presence of the polar species *Neogloboquadrina pachyderma* s. (Volkmann 2000), and the subpolar front species *Turborotalia quinqueloba* (Johannessen *et al.* 1994), the lowest abundances of the tropical-subtropical species *Orbulina universa* (Tolderlund and Bé 1971), and the high $\delta^{18}O$, all indicate relatively low temperatures. These cold sea surface temperatures (SSTs) are the consequence of a more southern latitudinal position of the polar front during the YD cold period (Pujol 1980; Eynaud *et al.* 2009; Thornalley *et al.* 2009, 2011; Penaud *et al.* 2011). *Turborotalia quinqueloba* may also reflect a well mixed water column (e.g. Bé and Tolderlund 1971, Kroon *et al.* 1991, Ortiz *et al.* 1995). Rather surprisingly, during this cold period a continuous presence (5–10%) of the tropical-subtropical *Globigerinoides ruber* (white) is recorded. Because *G. ruber* is nearly absent from living assemblages in the BoB (Retailleau *et al*. 2011), Mojtahid *et al.* (2013) suggested, on the basis of a study of a long core collected at the 550 m deep Station B (Fig. 1), that this species could be introduced into the BoB by the warm and salty Iberian Poleward and Navidad current (IPC and NC). Because the intensification of the NC is related to the combination of weak northerlies and strong south-southwesterly winds, which occurs under prevailing negative NAO conditions (Le Cann and Serpette 2009), Mojtahid *et al.* (2013) suggested the use of *G. ruber* as a proxy of negative NAO conditions. Following this hypothesis, the relatively high abundances of *G. ruber* in our early record suggests that the climatic context of the BoB during the YD was controlled by prevailing negative NAO conditions. After 11.2 cal ka BP, the proportions of the subtropical species *O. universa* (mainly observed today in the SE BoB during summer; Retailleau *et al*. 2011), gradually increase whereas the polar taxa (*N. pachyderma* s. and *T. quinqueloba*) decrease in response to the glacial-interglacial transition. The progressive warming of the SSTs is also perceptible in decreasing $\delta^{18}O$ values. Meanwhile, the progressive increase in $\delta^{13}C$ suggests enhanced surface water productivity, as it is corroborated by the clear transition from oligotrophic to mesotrophic conditions recorded by benthic foraminiferal assemblages.

2. During the 10.2–2.6 cal ka BP interval, planktic faunas are dominated by the temperate species *N. incompta, G. inflata* and *G. glutinata*. This indicates a northward migration of the sub-polar front (Eynaud *et al*. 2009) and a gradual establishment of the modern temperate surface waters in the BoB. However, the major faunal change in the proportion of these temperate species (a decrease of the percentage of *G. inflata* and an increase of *N. incompta*) is difficult to explain, since these two species have a rather similar temporal and spatial distribution in the modern NE Atlantic (Harbers *et al*. 2010, Retailleau *et al.* 2011). Mojtahid *et al.* (2013) found a similar turnover in the proportion of these two species at about the same time and argued that the decrease of *G. inflata* could be indicative of stronger water column stratification during summer. The increasing offset in $\Delta\delta^{18}O$ between *G. inflata* and *G. bulloides* during this period (Fig. 5) comforts the hypothesis of stronger water column stratification, probably due to warmer SSTs. During this time interval, *O. universa* records its highest abundances whereas

G. ruber shows fairly low values. The high percentages of *O. universa* between 8.4 and 4.8 cal ka BP may be indicative of maximum summer SSTs under the control of orbital forcing, i.e. the HTM. Meanwhile, the low proportion of *G. ruber* may indicate a generally prevailing positive NAO conditions, which agrees with other regional and global studies reconstructing Holocene NAO conditions (e.g. Lamb *et al.* 1989, Bernárdez *et al.* 2008a, Wanner *et al*. 2008); although the timing and the resolution are not always perfectly matching. At Station B, *G. ruber* records a peak between ~ 9 and 6 cal ka BP. This peak is totally absent from Station WH record. This discrepancy could be explained either by the low sedimentation rates at Station WH during this period or by restriction of the NC intrusion to the most southern part of the BoB. After 4.8 cal ka BP, *O. universa* progressively declined. This suggests a gradual SST cooling trend as recorded in most NH Holocene reconstructions (e.g. Marchal *et al.* 2002, Kim *et al*. 2004, Rimbu *et al.* 2004, Naughton *et al.* 2007, Mojtahid *et al.* 2013).

3. The 2.6–1.3 cal ka BP interval is characterized by high relative abundances of *G. ruber* with a distinct peak at ~ 2.4 cal ka BP, parallel to an abrupt increase in the $\delta^{18}O$ of the most surficial species *G. bulloides*. This abrupt increase may have been induced either by colder SSTs or more saline waters. Higher salinities could be explained by intrusions of the salty NC as suggested by the highest proportions of *G. ruber*. At the same time, an abrupt decrease in $\delta^{13}C$ indicates low productivity events and homogenization of the water column (low $\Delta\delta^{13}C$ and $\Delta\delta^{18}O$). After this event of a putative strongly negative NAO index (from ~ 2.6 to 2.0 cal ka BP), $\delta^{18}O_{G.\ bulloides}$ decreases simultaneously with decreasing proportions of *G. ruber* until ~ 1.3 cal ka BP, suggesting a progressive shift towards more positive NAO condition. The ~ 2.6 to 2.0 cal ka BP time interval, partially coincides with the Iberian-Roman Humid Period (2.6–1.6 cal ka BP), well recorded in high-resolution paleoclimate archives from the Iberian Peninsula, and characterized by increased precipitations under a prevailing negative NAO (e.g. Diz *et al*. 2002, Bernárdez *et al.* 2008b).

4. The last 1.3 cal ka BP are mainly characterized by high proportions of *G. inflata* which match the final increase in the proportions of the benthic species *U. peregrina*. This might suggest a period of enhanced surface productivity along the Iberian margin. Additionally, the gradual increase of *G. scitula* (a deep-dwelling species; e.g. Bé 1977), which was nearly absent before 2.2 cal ka BP, may indicate an increase in the availability of more labile organic matter in deep waters (Itou and Noriki 2002, Schiebel *et al.* 2002). The heavier values of $\delta^{13}C_{G.\ inflata}$ especially between 1.3 and 0.6 cal ka BP corroborates the latter hypothesis (Fig. 5). During the last 1.3 cal ka BP, *G. ruber* is nearly absent, which is consistent with the record at Station B (Fig. 1; Mojtahid *et al.* 2013). This suggests a weakening of the influence of the NC and a prevailing positive NAO index. This is consistent with the results of Martins *et al.* (2006a, b) that showed an enhanced upwelling activity off the Iberian coast since 2.2 cal ka BP due the intensification of northerly winds; under positive NAO conditions.

CONCLUSIONS

Because of our very good knowledge of the ecology of the modern foraminiferal faunas in the BoB, we are able to interpret the local paleoenvironmental signals recorded by fossil faunas in terms of global (orbital forcing) and regional (NAO, seasonality) climatic forcing. Over the last 12.8 cal ka BP, changes occurred in sedimentology, foraminiferal assemblages and their isotopic signatures in the SE BoB.

In the context of post-glacial sea level rise, the SE BoB has experienced enhanced turbidite activity through submarine canyons until 7.6 cal ka BP. From 12.8 to 10.2 cal ka BP, upper shelf material was supplied to the deep-sea environment by enhanced lateral advection, due to the low sea-level stand and the narrow continental shelf. In addition, relatively high abundances of *Globigerinoides ruber* suggest that the climatic context of the BoB, under prevailing negative NAO conditions, could have been more humid enhancing river runoff.

During the studied period, the trophic conditions in the BoB progressively shift from rather oligotrophic during the YD to more nutrient-enriched environments nowadays. Linked to more productive surface waters, an enhanced downward flux of organic matter leads to increased proportions of mesotrophic species, and a disappearance of oligotrophic benthic taxa. The planktic foraminiferal signal, mirrored by the benthic signal indicates a progressive increase in quantity and quality of nutrient supply into the BoB. After 7.6 cal ka, the BoB deep-sea environment obtains its modern configuration with dominantly hemipelagic deposits, and strong seasonality in primary and export production. This increased planktic ecosystem seasonality is responsible

for an increased organic matter flux to the seafloor. The ~ 2.6–1.3 cal ka BP interval is characterized by high nutrient supply as a consequence of increased river runoff, under prevailing negative NAO conditions as testified by the presence of *G. ruber*. The last 1.3 cal ka BP period shows an increase in the proportion of labile organic matter in the deep water column.

The external orbital forcing is perceptible through the SSTs records by planktic fauna proportions. After the YD cold period, the three main climatic phases of the Holocene, classically described in the literature, are traced: warm SSTs in the early Holocene, maximum temperatures at the HTM (8.4–4.8 cal ka BP) followed by a general cooling trend.

Sedimentary records from two distant sites (Site WH, this study and Site B, Mojtahid *et al.* 2013), located in different physiographic contexts, have recorded a similar climatic global signals. However, due to the more coastal location of Site B (550 m deep, only 50 km off the French coast), the continental influence is higher resulting in a more eutrophic environment. Nevertheless, the combination of this study and Mojtahid *et al.* (2013) gives for the first time, a fairly comprehensive spatial overview of the functioning of the BoB during the Holocene.

Acknowledgements. The authors are grateful to the editor and to the reviewers for the improvement of the manuscript. We would like to thank the crew members of the R/V "Côte de la Manche" (CNRS-INSU), and engineers of the Technical Department-INSU/CNRS for their help during the sampling campaign. We would like to thank also S. Terrien for her help with data processing, and the technical staff of EPOC for their help with sedimentological analyses. PECH 1 and CADIAC cruises were supported by the ANR FORCLIM (ANR-05-BLAN-02751). A 3-years doctoral fellowship was provided to J. Garcia by the Departmental Council of Vendée.

REFERENCES

Abrantes F., Lebreiro S., Rodrigues T., Gil I., Bartels-Jónsdóttir H., Oliveira P., Kissel C., Grimalt J. O. (2005) Shallow-marine sediment cores record climate variability and earthquake activity off Lisbon (Portugal) for the last 2000 years. *Quaternary Sci. Rev*. **24:** 2477–2494

Andersen C., Koç N., Jennings A., Andrews J. T. (2004) Nonuniform response of the major surface currents in the Nordic Seas to insolation forcing: Implications for the Holocene climate variability. *Paleoceanograph*. **19:** 2003–2019

Bé A. W. H., Tolderlund D. S. (1971) Distribution and ecology of living planktonic foraminifera in surface waters of the Atlantic and Indian Oceans. In: The Micropaleontology of Oceans, (Eds. B. M. Funnel and W. R. Riedel), Cambridge University Press, 105–149

Bé A. W. H. (1977) Ecology of planktonic foraminifera and biogeographic patterns of life and fossil assemblages in the Indian Ocean. *Micropaleontology* **23:** 369–414

Beaufort L., Heussner S. (1999). Coccolithophorids on the continental slope of the Bay of Biscay – production, transport and contribution to mass fluxes. *Deep-Sea Res*. Pt. II. **10:** 2147–2174

Bernárdez P., González-Álvarez R., Francés G., Prego R., Bárcena M. A., Romero O. E. (2008a) Late Holocene history of the rainfall in the NW Iberian peninsula – Evidence from a marine record. *J. Marine Syst*. **72:** 366–382

Bernárdez P., González-Álvarez R., Francés G., Prego R., Bárcena M. A., Romero O. E. (2008b) Palaeoproductivity changes and upwelling variability in the Galicia Mud Patch during the last 5000 years: geochemical and microfloral evidence. *The Holocene* **18:** 1207–1218

Berner R. A. (1980) Early diagenesis: A theoretical approach, Princeton University Press

Bizon G., Bizon J. J. (1984). Distribution des foraminifères sur le plateau continental au large du Rhône. In: Ecologie des microorganismes en Méditerranée occidentale 'ECOMED', (Eds. J. J. Bizon, P. F. Burollet), Association Française des Techniciens du Pétrole, Paris, 84–94

Bond G., Kromer B., Beer J., Muscheler R., Evans M. N., Showers W., Hoffmann S., Lotti-Bond R., Hajdas I., Bonani G. (2001) Persistent solar influence on North Atlantic climate during the Holocene. *Science* **294:** 2130–2136

Broecker W. S., Denton G. H., Edwards R. L., Cheng H., Alley R. B., Putnam A. E. (2010) Putting the Younger Dryas cold event into context. *Quaternary Sci. Rev*. **29:** 1078–1081

Bronk Ramsey C. (2008) Deposition models for chronological records. *Quaternary Sci. Rev*. **27:** 42–60

Bronk Ramsey C. (2009) Bayesian analysis of radiocarbon dates. *Radiocarbon* **51:** 337–360

Caralp M. (1971) Les foraminifères planctoniques du Pléistocène terminal dans le Golfe de Gascogne: interprétation biostratigraphique et paléoclimatique. Université I, Faculté des Sciences

Cléroux C., Debret M., Cortijo E., Duplessy J.-C., Dewilde F., Reijmer J., Massei N. (2012) High-resolution sea surface reconstructions off Cape Hatteras over the last 10 ka. *Paleoceanography* **27:** PA1205

Coplen T. B. (1988) Normalization of oxygen and hydrogen isotope data. *Chem. Geol.: Isotope Geoscience section* **72:** 293–297

Corliss B. H., Honjo S. (1981) Dissolution of deep-sea benthonic foraminifera. *Micropaleontology* **27:** 356–378

Dansgaard W., Johnsen S. J., Clausen H. B., Dahl-Jensen D., Gundestrup N. S., Hammer C. U., Hvidberg C. S., Steffensen J. P., Sveinbjörnsdottir A. E., Jouzel J. (1993) Evidence for general instability of past climate from a 250-kyr ice-core record. *Nature* **364:** 218–220

Darling K. F., Wade C. M. (2008) The genetic diversity of planktic foraminifera and the global distribution of ribosomal RNA genotypes. *Mar. Micropaleontol*. **67:** 216–238

Debret M., Sebag D., Crosta X., Massei N., Petit J.-R., Chapron E., Bout-Roumazeilles V. (2009) Evidence from wavelet analysis for a mid-Holocene transition in global climate forcing. *Quaternary Sci. Rev*. **28:** 2675–2688

Decastro M., Gómez-Gesteira M., Álvarez I., Crespo A. J. C. (2011) Atmospheric modes influence on Iberian Poleward Current variability. *Cont. Shelf Res*. **31:** 425–432

Diz P., Francés G., Pelejero C., Grimalt J. O., Vilas F. (2002) The last 3000 years in the Ría de Vigo (NW Iberian Margin): climatic and hydrographic signals. *The Holocene* **12:** 459–468

Duchemin G., Fontanier C., Jorissen F. J., Barras C., Griveaud C. (2007) Living small-sized (63–150 μm) foraminifera from mid-

shelf to mid-slope environments in the Bay of Biscay. *J. Foramin. Res*. **37:** 12–32

Duplessy J. C. (1978) Isotope studies. In: Climatic Change (Eds. J. Gribbin), Cambridge University Press, Cambridge, 46–67

Duros P., Fontanier C., Metzger E., Cesbron F. Deflandre B., Schmidt S., Buscail R., Zaragosi S., Kerhervé P., Rigaud S., Delgard M.-L., Jorissen M. J. (2013) Live (stained) benthic foraminifera from the Cap-Ferret Canyon (Bay of Biscay, NE Atlantic): A comparison between the canyon axis and the surrounding areas. *Deep-Sea Res*. Pt. I. **74:** 98–114

Duros P., Fontanier C., Metzger E., Pusceddu A., Cesbron F., de Stigger H. C., Bianchelli S., Danovaro R., Jorissen F. J. (2011) Living (stained) benthic foraminifera in the Whittard Canyon, Celtic margin (NE Atlantic). *Deep-Sea Res*. Pt. I. **58:** 128–146

Durrieu de Madron X., Castaing P., Nyffeler F., Courp T. (1999) Slope transport of suspended particulate matter on the Aquitanian margin of the Bay of Biscay. *Deep-Sea Res*. Pt. II. **46:** 2003–2027

Eynaud F., De Abreu L., Voelker A., Schönfeld J., Salgueiro E., Turon J.-L., Penaud A., Toucanne S., Naughton F., Sánchez Goñi M. F., Malaizé B., Cacho I. (2009) Position of the Polar Front along the western Iberian margin during key cold episodes of the last 45 ka. *Geochem., Geophys., Geosys*. **10:** Q07U05, doi:10.1029/2009GC002398

Fahl K., Stein R. (2012) Modern seasonal variability and deglacial/Holocene change of central Arctic Ocean sea-ice cover: New insights from biomarker proxy records. *Earth Planet. Sc. Lett*. **351**–**352:** 123–133

Faugères J.-C., Gonthier E., Mulder T., Kenyon N., Cirac P., Griboulard R., Berné S., Lesuavé R. (2002) Multi-process generated sediment waves on the Landes Plateau (Bay of Biscay, North Atlantic). *Mar. Geol*. **182:** 279–302

Fontanier C., Jorissen F. J., Chaillou G., Anschutz P., Grémare A., Griveaud C., (2005) Live foraminiferal faunas from a 2800 m deep lower canyon station from the Bay of Biscay: faunal response to focusing of refractory organic matter. *Deep-Sea Res*. Pt. I. **52:** 1189–1227

Fontanier C., Jorissen F., Chaillou G., David C., Anschutz P., Lafon V. (2003) Seasonal and interannual variability of benthic foraminiferal faunas at 550 m depth in the Bay of Biscay. *Deep-Sea Res*. Pt. I. **50:** 457–494

Fontanier C., Jorissen F., Licari L., Alexandre A., Anschutz P., Carbonel P. (2002) Live benthic foraminiferal faunas from the Bay of Biscay: faunal density, composition, and microhabitats. *Deep-Sea Res*. Pt. I. **49:** 751–785

Garcia-Soto C., Pingree R. D., Valdes L. (2002) Navidad development in the southern Bay of Biscay: Climate change and swoddy structure from remote sensing and in situ measurements. *J. Geophys. Res*. **107:** 28.1–28.29

Goldstein S. T., Corliss B. H. (1994) Deposit feeding in selected deep-sea and shallow-water benthic foraminifera. *Deep-Sea Re*s. Pt. II. **41:** 229–241

Gooday A. J. (2003) Benthic foraminifera (Protista) as tools in deep-water palaeoceanography: environmental influences on faunal characteristics. *Adv. Mar. Biol*. **46:** 1–90

Harbers A., Schönfeld J., Rüggeberg A., Pfannkuche O. (2010) Short term dynamics of planktonic foraminiferal sedimentation in the Porcupine Seabight. *Micropaleontology* **56:** 259–274

Herguera J. C. (1992) Deep-sea benthic foraminifera and biogenic opal: glacial to postglacial productivity changes in the western equatorial Pacific. *Mar. Micropaleontol*. **19:** 79–98

Herguera J. C., Berger W. H. (1991) Paleoproductivity from benthic foraminifera abundance: Glacial to postglacial change in the west-equatorial Pacific. *Geology* **19:** 1173–1176

Hua Q., Barbetti M. (2004) Review of tropospheric bomb ^{14}C data for carbon cycle modeling and age calibration purposes. *Radiocarbon* **46:** 1273–1298

Itou M., Noriki S. (2002) Shelf fluxes of solution-resistant planktonic foraminifers as a proxy for mixed-layer depth. *Geoph. Res. Lett*. **29:** 19-1–19-4

Jorissen F. J., De Stigter H. C., Widmark J. G. (1995) A conceptual model explaining benthic foraminiferal microhabitats. *Mar. Micropaleontol*. **26:** 3–15

Jorissen F. J., Fontanier C., Thomas E. (2007) Chapter Seven Paleoceanographical Proxies Based on Deep-Sea Benthic Foraminiferal Assemblage Characteristics. *Dev. Mar. Geol*. **1:** 263–325

Jorissen F. J., Wittling I. (1999) Ecological evidence from live-dead comparisons of benthic foraminiferal faunas off Cape Blanc (Northwest Africa). *Palaeogeogr. Palaeocl*. **149:** 151–170

Johannessen T., Jansen E., Flatøy A., Ravelo A. C. (1994) The relationship between surface water masses, oceanographic fronts, and paleoclimatic proxies in surface sediments of the Greenland, Iceland, Norwegian Seas. *Nato ASI Series* **117:** 61–85

Kaufman D., Ager T., Anderson N., Anderson P., Andrews J., Bartlein P., Brubaker L., Coats L., Cwynar L., Duvall M., Dyke A., Edwards M., Eisner W., Gajewski K., Geirsdóttir A., Hu F., Jennings A., Kaplan M., Kerwin M., Lozhkin A., MacDonald G., Miller G., Mock C., Oswald W., Otto-Bliesner B., Porinchu D., Rühland K., Smol J., Steig E., Wolfe B. (2004) Holocene thermal maximum in the western Arctic (0–180°W). *Quaternary Sci. Rev*. **23:** 529–560

Kim J. H., Rimbu N., Lorenz S. J., Lohmann G., Nam S. I., Schouten S., Rühllemann C., Schneider R. R. (2004) North Pacific and North Atlantic sea-surface temperature variability during the Holocene. *Quaternary Sci. Rev*. **23:** 2141–2154

Koutsikopoulos C., Le Cann B. (1996) Physical processes and hydrological structures related to the Bay of Biscay anchovy. *Sci. Mar*. **60:** 9–19

Kroon D., Steens T., Troelstra S. R. (1991) 13. Onset of monsoonal upwelling in western Arabian Seas as revealed by planktonic foraminifers. In: *Proc. ODP*, *Sci. Results*, College Station, TX (Ocean Drilling Program), (Eds. W. L. Prell, N. Niitsuma *et al*.), **117:** 257–263

Kuhnt T., Howa H., Schmidt S., Marié L., Schiebel R. (2013) Flux dynamics of planktic foraminiferal tests in the south-eastern Bay of Biscay (northeast Atlantic margin). *J. Marine Syst*. **109**–**110:** 169–181

Lamb H. F., Eicher U., Switsur V. R. (1989) An 18,000-year record of vegetation, lake-level and climatic change from Tigalmamine, Middle Atlas, Morocco. *J. Biogeogr*. **16:** 65–74

Lambeck K., Yokoyama Y., Purcell T. (2002) Into and out of the Last Glacial Maximum: sea-level change during Oxygen Isotope Stages 3 and 2. *Quaternary Sci. Rev*. **21:** 343–360

Lampert L. (2001) Dynamique saisonnière et variabilité pigmentaire des populations phytoplanctoniques dans l'Atlantique Nord (Golfe de Gascogne). Ph.D. Thesis, Université de Bretagne occidentale, Brest, France

Le Cann B., Serpette A. (2009) Intense warm and saline upper ocean inflow in the southern Bay of Biscay in autumn–winter 2006–2007. *Cont. Shelf Res*. **29:** 1014–1025

Liu K. K., Dittert N. (2010) Web-based electronic supplements, Appendix C. In: Carbon and Nutrient Fluxes in Continental Mar-

gins, (Eds. K. K. Liu, L. Atkinson, R. A. Quiñones, L. Talaue-McManus). Springer, Berlin http://cmtt.pangaea.de/ [October 2, 2012]

Longhurst A. R. (2007) Ecological geography of the sea. Academic Press

Loubere P., Gary A. (1990) Taphonomic process and species microhabitats in the living to fossil assemblage transition of deeper water benthic foraminifera. *Palaios* **5:** 375–381

Marchal O., Cacho I., Stocker T. F., Grimalt J. O., Calvo E., Martrat B., Shackleton N., Vautravers M., Cortijo E., Van Kreveld S., Andersson C., Koç N., Chapman M., Sbaffi L., Duplessy J.-C., Sarnthein M., Turon J.-L., Duprat J., Jansen E. (2002) Apparent long-term cooling of the sea surface in the northeast Atlantic and Mediterranean during the Holocene. *Quaternary Sci. Rev*. **21:** 455–483

Martins V., Jouanneau J. M., Weber O., Rocha F. (2006a) Tracing the late Holocene evolution of the NW Iberian upwelling system. *Mar. Micropaleontol*. **59:** 35–55

Martins V., Patinha C., Ferreira da Silva E., Jouanneau J. M., Weber O., Rocha F. (2006b) Holocene record of productivity in the NW Iberian continental shelf. *J. Geochem. Explor*. **88:** 408–411

Mayewski P. A., Rohling E. E., Curt Stager J., Karlén W., Maasch K. A., David Meeker L., Meyerson E. A., Gasse F., Van Kreveld S., Holmgren K., Lee-Thorp J., Rosqvist G., Rack F., Staubwasser M., Schneider R. R., Steig E. J. (2004) Holocene climate variability. *Quaternary Res*. **62:** 243–255

Migeon S., Weber O., Faugeres J.-C., Saint-Paul J. (1998) SCOPIX: a new X-ray imaging system for core analysis. *Geo-Mar. Lett.* **18:** 251–255

McCave I. N., Manighetti B., Robinson S. G., (1995) Sortable silt and fine sediment size/composition slicing: Parameters for palaeocurrent speed and palaeoceanography. *Palaeoceanograph*. **10:** 593–610

Mojtahid M., Griveaud C., Fontanier C., Anschutz P., Jorissen F. J. (2010) Live benthic foraminiferal faunas along a bathymetrical transect (140–4800 m) in the Bay of Biscay (NE Atlantic). *Rev. Micropal*. **53:** 139–162

Mojtahid M., Frans J., Garcia J., Schiebel R., Michel E., Eynaud F., Gillet H., Cremer M., Ferreiro P. D., Siccha M., Howa H. (2013) High resolution Holocene record in the southeastern Bay of Biscay: global versus regional signals. *Palaeogeogr. Palaeocl.* **377:** 28–44

Mouret A., Anschutz P., Deflandre B., Chaillou G., Hyacinthe C., Deborde J., Etcheber H., Jouanneau J.-M., Grémare A., Lecroart P. (2010) Oxygen and organic carbon fluxes in sediments of the Bay of Biscay. *Deep-Sea Res*. Pt. I. **57:** 528–540

Murray J. W. (2006) Ecology and applications of benthic foraminifera. Cambridge University Press

Murray J. W., Alve E. (1999) Natural dissolution of modern shallow water benthic foraminifera: taphonomic effects on the palaeoecological record. *Palaeogeogr. Palaeocl*. **146:** 195–209

Naughton F., Bourillet J. F., Sánchez Goñi M. F., Turon J. L., Jouanneau J. M. (2007) Long-term and millennial-scale climate variability in northwestern France during the last 8850 years. *The Holocene* **17:** 939–953

Oldfield F. (2003) Introduction: the Holocene, a special time. In: Global Change in the Holocene, (Eds. A. Mackay, R. Battarbee, J. Birks, F. Oldfield). Arnold, London, 1–9

Oppo D. W., McManus J. F., Cullen J. L. (2003) Palaeo-oceanography: Deepwater variability in the Holocene epoch. *Nature* **422:** 277–277

Ortiz J. D., Mix A. C., Collier R. W. (1995) Environmental control of living symbiotic and asymbiotic foraminifera of the California Current. *Paleoceanograph*. **10:** 987–1009

Pena L. D., Francés G., Diz P., Esparza M., Grimalt J. O., Nombela M. A., Alejo I. (2010) Climate fluctuations during the Holocene in NW Iberia: High and low latitude linkages. *Cont. Shelf Res*. **30:** 1487–1496

Penaud A., Eynaud F., Voelker A., Kageyama M., Marret F., Turon J.-L., Blamart D., Mulder T., Rossignol L. (2011) Assessment of sea surface temperature changes in the Gulf of Cadiz during the last 30 ka: implications for glacial changes in the regional hydrography. *Biogeosciences* **8:** 2295–2316

Pingree R. D., Le Cann B. (1992) Three anticyclonic Slope Water Oceanic eDDIES (SWODDIES) in the southern Bay of Biscay in 1990. *Deep-Sea Res*. **39:** 1147–1175

Polyak L., Alley R. B., Andrews J. T., Brigham-Grette J., Cronin T. M., Darby D. A., Dyke A. S., Fitzpatrick J. J., Funder S., Holland M. (2010) History of sea ice in the Arctic. *Quaternary Sci. Rev*. **29:** 1757–1778

Puillat I., Lazure P., Jegou A.-M., Lampert L., Miller P. I. (2004) Hydrographical variability on the French continental shelf in the Bay of Biscay, during the 1990s. *Cont. Shelf Res*. **24:** 1143–1163

Pujol C. (1980) Les foraminifères planctoniques de l'Atlantique Nord au Quaternaire. Ecologie-Stratigraphie-Environnement. Université Bordeaux I, 254

Reimer P. J., Baillie M. G., Bard E., Bayliss A., Beck J. W., Blackwell P. G., Ramsey C. B., Buck C. E., Burr G. S., Edwards R. L. (2009) IntCal09 and Marine09 radiocarbon age calibration curves, 0–50,000 years cal BP. *Radiocarbon* **51:** 1111–1150

Retailleau S., Eynaud F., Mary Y., Abdallah V., Schiebel R., Howa H. (2012) Canyon heads and river plumes: How might they influence neritic planktonic foraminifera communities in the SE Bay of Biscay? *J. Foramin. Res*. **42:** 257–269

Retailleau S., Howa H., Schiebel R., Lombard F., Eynaud F., Schmidt S., Jorissen F., Labeyrie L. (2009) Planktic foraminiferal production along an offshore-onshore transect in the southeastern Bay of Biscay. *Cont. Shelf Res*. **29:** 1123–1135

Retailleau S., Schiebel R., Howa H. (2011) Population dynamics of living planktic foraminifers in the hemipelagic southeastern Bay of Biscay. *Mar. Micropaleontol*. **80:** 89–100

Rimbu N., Lohmann G., Lorenz S. J., Kim J. H., Schneider R. R. (2004) Holocene climate variability as derived from alkenone sea surface temperature and coupled ocean-atmosphere model experiments. *Clim. Dynam*. **23:** 215–227

Ruddiman W. F., Ellis E. C. (2009) Effect of per-capita land use changes on Holocene forest clearance and CO_2 emissions. *Quaternary Sci. Rev*. **28:** 3011–3015

Schiebel R., Schmuker B., Alves M., Hemleben C. (2002) Tracking the recent and Late Pleistocene Azores front by the distribution of planktic foraminifers. *J. Mar. Syst*. **37:** 213–227

Schmidt S., Howa H., Mouret A., Lombard F., Anschutz P., Labeyrie L. (2009) Particle fluxes and recent sediment accumulation on the Aquitanian margin of Bay of Biscay. *Cont. Shelf Res*. **29:** 1044–1052

Stow D. A. V., Piper D. J. W. (1984) Deep-water fine-grained sediments: facies models. Geolog. Soc., London, Special Publications **15:** 611–646

Thornalley D. J. R., Elderfield H., McCave I. N. (2009) Holocene oscillations in temperature and salinity of the surface subpolar North Atlantic. *Nature* **457:** 711–714

Thornalley D. J. R., Elderfield H., McCave I. N. (2011) Reconstructing North Atlantic deglacial surface hydrography and its link to the Atlantic overturning circulation. *Global Planet. Change* **79:** 163–175

Tisnérat-Laborde N., Poupeau J. J., Tannau J. F., Paterne M. (2001) Development of a semi-automated system for routine preparation of carbonate samples. *Radiocarbon* **43:** 299–304

Tolderlund D. S., Bé A. W. (1971) Seasonal distribution of planktonic foraminifera in the western North Atlantic. *Micropaleontology* **17:** 297–329

Toucanne S., Zaragosi S., Bourillet J.-F., Naughton F., Cremer M., Eynaud F., Dennielou B. (2008) Activity of the turbidite levees of the Celtic-Armorican margin (Bay of Biscay) during the last 30,000 years: imprints of the last European deglaciation and Heinrich events. *Mar. Geol*. **247:** 84–103

van Aken H. M. (2000a) The hydrography of the mid-latitude northeast Atlantic Ocean: I: The deep water masses. *Deep-Sea Res*. Pt. I. **47:** 757–788

van Aken H. M. (2000b) The hydrography of the mid-latitude Northeast Atlantic Ocean: II: The intermediate water masses. *Deep-Sea Res*. Pt. I. **47:** 789–824

van Aken H. M. (2001) The hydrography of the mid-latitude Northeast Atlantic Ocean: III: The subducted thermocline water mass. *Deep-Sea Res*. Pt. I. **48:** 237–267

van Aken H. M. (2002) Surface currents in the Bay of Biscay as observed with drifters between 1995 and 1999. *Deep-Sea Res*. Pt. I. **49:** 1071–1086

Volkmann R. (2000) Planktic foraminifers in the outer Laptev Sea and the Fram Strait – Modern distribution and ecology. *J. Foramin. Res*. **30:** 157–176

Walton W. R.(1952) Techniques for recognition of living foraminifera. *J. Foramin. Res*. **3:** 56–60

Wanner H., Beer J., Bütikofer J., Crowley T. J., Cubasch U., Flückiger J., Goosse H., Grosjean M., Joos F., Kaplan J. O. (2008) Mid-to Late Holocene climate change: an overview. *Quaternary Sci. Rev*. **27:** 1791–1828

Received on 3rd March, 2013; revised on 23 May, 2013; accepted on 29th May, 2013